STOMACH-SPECIFIC CALPAIN, nCL-2, LOCALIZES IN MUCUS CELLS AND PROTEOLYZES THE β-SUBUNIT OF COATOMER COMPLEX, β-COP

Shoji Hata[1], Suguru Koyama[1, 2], Hiroyuki Kawahara[3], Naoko Doi[1, 4], Tatsuya Maeda[4, 5], Noriko Toyama-Sorimachi[6], Keiko Abe[2], Koichi Suzuki[7], Hiroyuki Sorimachi[1, 4]

[1]Department of Enzymatic Regulation for Cell Functions, The Tokyo Metropolitan Institute of Medical Science (Rinshoken), Tokyo 113-8613, [2]Graduate School of Agricultural and Life Sciences, University of Tokyo, Tokyo 113-8657, [3]Graduate School of Pharmaceutical Sciences, Hokkaido University, Hokkaido 060-0812, [4]CREST, Japan Science and Technology (JST), Saitama 332-0012, [5]Institute of Molecular and Cellular Biosciences, University of Tokyo, Tokyo 113-0032, [6]Department of Gastroenterology, Research Institute, International Medical Center of Japan, Tokyo 162-8655, and [7]New Frontiers Research Laboratories, Toray Industries Inc., Kanagawa 248-8555, Japan

Running title: Possible function of stomach-specific calpain

Correspondence to Hiroyuki Sorimachi: Department of Enzymatic Regulation for Cell Functions, Rinshoken, 3-18-22 Honkomagome, Bunkyo-ku, Tokyo 113-8613, Japan; E-mail: sorimach@rinshoken.or.jp; TEL/FAX: +81-3-3823-2181.

Calpain is a Ca^{2+}-regulated cytosolic protease. Mammals have 14 calpain genes, half of which are predominantly expressed in specific organ(s); the rest are expressed ubiquitously. A defect in calpains causes lethality/pathogenicity, indicating their physiological indispensability. nCL-2/calpain-8a was identified as a stomach-specific calpain, whose physiological functions are unclear. To elucidate these, we characterized nCL-2 in detail. Unexpectedly, nCL-2 was localized strictly to the surface mucus cells in the gastric epithelium and the mucus-secreting goblet cells in the duodenum. Yeast two-hybrid screening identified several nCL-2-intracting molecules. Of these, the β-subunit of coatomer complex (β-COP) occurs in the stomach pit cells and is proteolyzed by nCL-2 in vitro. Furthermore, β-COP and nCL-2 co-expressed in COS7 cells co-localized in the Golgi, and Ca^{2+}-ionophore stimulation caused the proteolysis of β-COP near the linker region, resulting in the dissociation of β-COP from the Golgi. These results strongly suggest novel functions for nCL-2 that involve the membrane trafficking of mucus cells via interactions with coat protein.

Calpain (EC 3.4.22.17) is an

intracellular Ca^{2+}-regulated cysteine protease, comprising a superfamily in most organisms including some bacteria, budding yeasts, fungi, plants, and animals. Calpains proteolyze specific substrates at very limited sites to irreversibly modify/modulate their functions, structures, and activities, and are thus called “modulator proteases”. Fourteen calpain genes have been identified in humans and mice and can be classified into two categories according to their expression, i.e., ubiquitous or tissue-specific (1,2,3). Ubiquitous μ- and m-calpains, two major calpains in mammals, form a heterodimer composed of a distinct 80 kDa catalytic large subunit (abbreviated to “μCL” and “mCL”, respectively) and a common 30 kDa regulatory small subunit (30K). Calpain three-dimensional structures define four (I–IV) and two (V and VI) domains in the large and small subunits, respectively: the regulatory N-terminal domain (I), the protease domain (II), the C2-domain-like Ca^{2+}/phospholipid-binding domain (III), the penta-EF-hand domains (IV and VI), and the Gly-clustering domain (V) (4,5). In the absence of Ca^{2+}, the protease domain (II) is further divided into two subdomains, IIa and IIb, which form a single active domain upon binding to Ca^{2+} (6,7).

Genetic studies in mammals and other organisms have clearly shown the physiological indispensability of the calpains. A gene knock-out mouse with a mutation in the gene for 30K, *Capn4*, exhibits embryonic lethality (8); mutations in the human gene for skeletal-muscle-specific p94/calpain 3, *CAPN3*, are responsible for limb-girdle muscular dystrophy type 2A (9); and a single nucleotide polymorphism in intron 3 of the human gene for calpain 10, *CAPN10*, is associated with type 2 diabetes (10). Mutations in the calpain genes of various other organisms, including yeasts, plants, nematodes, and *Drosophila*, result in significant phenotypes corresponding to defects in stress responses, sex determination, organogenesis, etc. (11,12,13,14,15). However, our understanding of the specific molecular mechanisms underlying calpain functions *in vivo* is far from complete.

One clue to the molecular actions of calpain is their tissue-specificity, because this should reflect their specific cellular functions, which are highly differentiated and specialized in the corresponding tissues. Indeed, a defect in skeletal-muscle-specific calpain causes muscular dystrophy, as mentioned above. nCL-2, also called calpain 8a, is another tissue-specific calpain, which is predominantly expressed in the stomach (16). The domain structure of nCL-2 is identical to that of mCL described above. By alternative splicing, the gene for nCL-2, *Capn8*, generates nCL-2´ (also called calpain 8b), which lacks domains III and IV (16,17). Possible functions have been reported for nCL-2 in the pituitary gland and for its *Xenopus laevis* homologue, XCL-2, in embryogenesis (18,19). However, the specific targets and functions of nCL-2 are still unclear.

Another tissue-specific calpain, nCL-4, the expression of which is predominantly in the digestive tract, also occurs in the stomach. It is reported to be down-regulated in a subset of gastric cancer patients and is involved in the suppression of tumorigenesis (20,21,22). μ-Calpain is also involved in the acid secretory process by cleaving ezrin, a membrane cytoskeletal protein, in parietal cells (23). How these data relate to the physiological functions of nCL-2/-2´ has yet to be elucidated.

The stomach is a highly differentiated organ with specific functions and complex programmed glandular structures, organized into diverse types of epithelial cells. The rodent stomach is composed of four regions: fundus, cardia, corpus, and pylorus, the latter three of which have numerous tubular pits with glands deep within them (24). The pits are lined by pit cells that secrete neutral mucus to protect the epithelium from acid (25). The oxyntic glands in the corpus consist of acid-secreting parietal cells, pepsinogen-secreting chief cells, and hormone-secreting enteroendocrine cells (25,26). Pylorocytes and gastrin-secreting G cells are mainly found in the pyloric glands of the pylorus (27). All these cells originate from proliferative progenitor cells located under the pits and undergo continuous renewal. The progenitor cells follow a specific differentiation process during their migration upwards, downwards, or both, to their final programmed destinations (25). Therefore, to understand nCL-2 functions, it is essential first to determine its localization in the stomach. In this study, *in situ* hybridization (ISH) and immunohistochemical analysis of nCL-2/-2´ were performed to localize them precisely. Surprisingly, nCL-2 was strictly localized in the pit cells, in sharp contrast to the expression of the ubiquitous calpains. Furthermore, yeast two-hybrid screening followed by biochemical analysis demonstrated the proteolytic interaction between nCL-2 and the β-subunit of the COPI coatomer complex (β-COP), strongly suggesting novel functions for nCL-2 that involve the membrane trafficking of mucus cells by interacting with coat proteins.

MATERIALS AND METHODS

Materials – Adult male Wistar rats and C57BL6/J mice were sacrificed by cervical dislocation to obtain tissue samples for ISH and immunohistochemistry. Tissue samples were removed, washed in ice-cold PBS, sliced, embedded in Tissue-Tek O.C.T. compound (Sakura Finetechnical Inc., Tokyo, Japan), and frozen in liquid nitrogen. Sections (7 μm thick) cut by cryostat were placed on glass slides coated with 3-aminopropyltriethoxysilane (Matsunami Glass Inc., Osaka, Japan). For immunocytochemistry, COS7 cells were plated onto Lab-tek chamber slides (Nalge Nunc International Inc.). For western blot analysis, the gastric mucosa was scraped from the stomach and homogenized in buffer A (20

mM Tris-Cl ,pH 8.0, 5 mM EDTA, and 1 mM DTT) containing 0.2 mM PMSF, 10 μg/ml aprotinin, and 50 μM pepstatin A. The supernatant recovered by centrifugation (20,000 × g, 30 min, 4°C) was used as the protein sample. μ-Calpain was prepared as described previously (28).

ISH – cDNA fragments encoding mouse nCL-2 (2,020 bp, nt 250–2269), mouse nCL-4 (1,369 bp, nt 700–2068), mouse mCL (1,491 bp, nt 700–2190), and mouse μCL (1,555 bp, nt 700–2254) were amplified by PCR using a mouse 17-day embryo cDNA library (CLONTECH Inc., ML4013AH) or mouse stomach first-strand cDNA and the following sets of primers: (nCL2-s) 5′-ctggacaaactcaaggcatcatctggaa-3′ and (nCL2-as) 5′-agggaagttgttgatgtccagagggtc-3′; (nCL4-s) 5′-gctctagataccctgaatgcctcagaatctgaa-3′ and (nCL4-as) 5′-gcggatcctcagatgttcatggtcaggctgatg-3′; (mCL-s) 5′-gctctagaaggctttggagaaaggttctctgct-3′ and (mCL-as) 5′-gcggatcctcaaggtccagatacaaagtgtcta-3′; (μCL-s) 5′-gctctagacctgcagaaggccccc-3′ and (μCL-as) 5′-gcggatcctcaggcaaacatagtcagctggagc-3′.

The amplified fragments were subcloned into the pBluescript SK(–) vector. Digoxigenin (Dig)-labeled riboprobes were synthesized and hybridized according to the manufacturer's manual for nonradioactive *in situ* hybridization (Roche Inc.).

Antibodies – Anti-nCL2/2′ and -nCL2C antibodies were raised in rabbits and affinity-purified using recombinant rat nCL-2′ (full-length) and an nCL-2-specific region (amino acids 379–713), respectively. Anti-H^+/K^+-ATPase β-subunit monoclonal antibody (clone 2G11), anti-PCNA monoclonal antibody (clone PC-10), anti-GM130 monoclonal antibody (clone 35), anti-β-COP antibody and anti-FLAG monoclonal antibody (clone M2) were purchased from Sigma, Neomarkers, BD Biosciences, Affinity Bioreagents and Stratagene Inc., respectively. Alexa 488-conjugated goat anti-mouse and Alexa 594-conjugated goat anti-rabbit IgGs were from Invitrogen Inc.

Immunostaining – Stomach sections and COS7 cells prepared as described above were fixed with 4% paraformaldehyde in PBS. After incubation with 5% normal goat serum, 1% BSA, and 0.1% Triton X-100 in PBS, they were incubated with primary antibody at 4°C overnight, and then with secondary antibody at room temperature for 30 min. An HRP-catalyzing method using the Vectastain Elite ABC kit (Vector Laboratories Inc.) and 3,3′-diazobenzidine hydrochloride or an immunofluorescence method using Alexa-labeled secondary antibodies was used to detect the bound antibodies.

Northern blot analyses – Mouse RNAs were isolated and blotted onto nylon membranes as described previously (16). For human tissues, RNA-blotted membrane was purchased from CLONTECH Inc. (nos. 636818 and 636835). Probes were prepared

from cDNA clones for mouse and human nCL-2, mouse nCL-2´, mCL, and glyceraldehyde phosphate dehydrogenase (GAPDH), and bands were detected as previously described (16).

Yeast two-hybrid analyses – Full-length mouse nCL-2 or domain IV (corresponding to amino acids 533–713) was cloned into pGBKT7 (CLONTECH Inc.) and used as bait. The bait plasmid and then a mouse 17-day embryo cDNA library (ML4013AH) were transformed into *Saccharomyces cerevisiae* AH109, according to the manufacturer's instructions. Cells were plated onto SD-LWHA plates and incubated at 30°C. Prey plasmids were recovered from the grown colonies by transformation of the isolated total yeast DNA into *E. coli*, and the sequences were determined.

Cloning and construction of expression plasmids – Mouse stomach total RNA was extracted from an adult male mouse (C57BL6/J) using Trizol reagent (Invitrogen Inc.). First-strand cDNAs were reverse-transcribed from 5 μg of total RNA using a First-Strand cDNA Synthesis Kit (Amersham Biosciences Inc.). Mouse nCL-2, β-COP, Eya2, GPS1, nm23-M2, and nm23-M4 cDNAs were amplified by PCR using *Pfu* DNA polymerase (Stratagene Inc.) and the synthesized first-strand cDNAs described above. The β-COP deletion mutant, β-COP-C (amino acids 529–953) cDNAs, was prepared by PCR using *Pfu* DNA polymerase and the full-length β-COP cDNA. For bacterial expression, cDNAs were inserted into the pCold I vector (TaKaRa Inc., Kyoto, Japan) to produce proteins with an N-terminal His-tag. For COS7 cell transfections, cDNAs were inserted into pSRD (29) to produce proteins with an N-terminal FLAG or HA tag.

Protein expression and purification – The *E. coli* expression plasmids constructed as described above were transformed into *E. coli* BL21/pG-Tf2 (TaKaRa Inc.), and the transformants were cultured at 37°C in 500 ml of LB medium containing 0.1 mg/ml ampicillin and 5 ng/ml tetracycline to A_{600} = 0.5. Protein expression was induced by the addition of 0.5 mM IPTG for 24 h at 15°C. Harvested cells were suspended in 40 ml of buffer B (20 mM Tris-Cl , pH 7.5 and 150 mM NaCl), and lysed with a French press (American Instrument Inc.). The supernatant was recovered by ultracentrifugation (105,000 × g, 30 min, 4°C), and filtered through 0.22 μm pore filter (Millipore Inc.). The supernatant was then applied to a 2 ml Ni^{2+}-chelating agarose column (Qiagen Inc.) equilibrated with buffer B. The column was washed with 20 mM imidazole in buffer B and eluted with 200 mM imidazole in buffer B. The eluent was further purified by MiniQ anion-exchange column (Amersham Biosciences Inc.) chromatography with a linear gradient of 0–0.5 M NaCl in 10 mM Tris-Cl (pH 7.5), 1 mM EDTA, and 1 mM DTT. Purification was confirmed by SDS-PAGE for its homogeneity. The purified protein was stored at 4°C until use.

Proteolysis assay – The pSRD constructs were transfected into COS7 cells by electroporation, as previously described (29). For the *in vitro* assay, COS7 cells were harvested 48 h after transfection, suspended in buffer A, and lysed by sonication. The lysates were then incubated with a final concentration of 5 mM Ca^{2+} or EDTA for 30 min at 30°C. The reactions were stopped by the addition of 6 × SDS sample buffer. For the cell culture assay, cells were treated with medium containing 10 μM Ca^{2+} ionophore, A23187, 48 h after transfection. Cells were harvested 20 h after A23187 treatment (at this point, cells were not significantly damaged under our culture conditions), suspended in buffer A, and lysed by sonication. The lysates were mixed with 6 × SDS sample buffer and boiled. The samples were used for SDS–PAGE and western blot analysis.

Immunoprecipitation and GST pull-down – For immunoprecipitation, transfected COS7 cells were harvested 48 h after transfection and lysed with lysis buffer (buffer A containing 5 mM EDTA, 0.5% nonidet P-40 (NP-40), 0.2 mM PMSF, and 10 μg/ml aprotinin). The supernatants were recovered by centrifugation at 20,000 × g for 15 min and incubated with a 50% slurry of FLAG (M2) agarose (Sigma Inc.) for 2 h. Immunoprecipitated proteins were eluted with 0.1 mg/ml FLAG peptide and mixed with SDS sample buffer. TOM70 cDNA identified by yeast two-hybrid screening was subcloned into pGEX-5X to produce a GST-fusion protein. The cell lysate supernatant of COS7 cells transfected with FLAG-tagged mouse nCL-2:C105S was prepared by homogenizing cells with lysis buffer and centrifugation at 20,000 × g for 15 min. The supernatant was incubated with 5 μg of GST or GST–TOM70 immobilized on glutathione–Sepharose 4B (Amersham Biosciences Inc.) for 3 h at 4°C. The beads were washed five times with lysis buffer, and mixed with SDS sample buffer.

Protein sequencing – After SDS–PAGE, the proteins were blotted onto Pro-Blot membrane (Applied Biosystems Inc.). Target protein bands on the membrane were visualized by Coomassie Brilliant Blue G-250 staining, excised, and washed three times with 0.1% (v/v) trifluoroacetic acid in 50% (v/v) methanol and then with absolute methanol. Sequencing was performed with the ABI 491cLC protein sequencer (Applied Biosystems Inc.) according to the manufacturer's instructions.

RESULTS

nCL-2 is expressed specifically in the pit cells of the gastric mucosa – To investigate the localization of nCL-2/-2′ expression in the stomach, *in situ* hybridization (ISH) analysis of the corpus and pylorus of the mouse stomach was performed. nCL-2/-2′ was expressed around the upper quarter of the corpus (oxyntic) mucosa and the upper half of the pyloric mucosa, where the mucus-secreting pit cells are abundant (Figs. 1A, B, 2A, B), whereas μCL and mCL

transcripts were detected in all cells including proliferative cells of the pyloric mucosa (Figs 1D, E, 2D, E). The digestive-tract-specific calpain, nCL-4, showed expression similar to but a little wider than that of nCL-2 (Figs. 1C, 2C).

The stomach was analyzed using anti-nCL2/2′ (reactive to both nCL-2 and -2′) and anti-nCL2C (reactive only to nCL-2) antibodies (Fig. 3A). Firstly, western blot analysis using protein extract from the gastric mucosa showed that the anti-nCL2/2′ antibody recognized nCL-2 but not nCL-2′ (Fig. 3B), indicating undetectable or no expression of nCL-2′ protein in the gastric mucosa, even though the amounts of nCL-2 and -2′ mRNAs in the stomach were similar (see Fig. 4A) (16). Consistently, immunohistochemical analysis showed that anti-nCL2/2′ and anti-nCL2C antibodies identified identical signals (Figs. 3C, D), suggesting that signals for nCL-2′ were also undetectable *in situ*.

The localization of nCL-2 protein was consistent with that observed by ISH (Figs. 3C–F). Significantly, nCL-2 signals were positive in the relatively smaller cells in the pits, and were absent from larger cells (Fig. 3F, arrowheads), which are considered to be the parietal cells located in the pit region (25). To confirm this, stomach sections were doubly immunostained with antibody directed against H^+/K^+-ATPase (green cells in Fig. 3G), a marker protein for parietal cells, or one directed against proliferating-cell nuclear antigen (PCNA) (green in Fig. 3H), a marker for progenitor cells. These signals did not overlap with that of nCL-2, indicating that nCL-2 is localized specifically in the pit cells and is thus implicated in pit cell functions.

nCL-2 is expressed in a subset of goblet cells in the small intestine – Northern blot analysis of human and mouse tissues with long exposures revealed that the gene for nCL-2 is expressed at low levels in the trachea and intestines (Fig. 4A). Therefore, these tissues were treated with ISH to detect the expression of nCL-2 and nCL-4 mRNAs. Signals were observed in some epithelial cells scattered in the villi of the duodenum (Figs. 4B, C). Furthermore, the nCL-2-positive cells were scattered in the upper half of the villi close to the luminal surface (Fig. 4B), whereas most of the nCL-4-positive cells were in the lower regions close to the crypt (Fig. 4C). Immunohistochemical analysis using anti-nCL2/2′ antibody showed patterns consistent with those obtained with ISH (Fig. 4D). The nCL2/2′-positive cells had an expanded shape in the apical region and were stained in the basal region. Their scattered distribution and the shape of the cells in the intestinal epithelium indicate that they correspond to mucus-secreting goblet cells. ISH and immunohistochemical analysis of the trachea, esophagus, and small and large intestines produced no significant signals (unpublished data), probably because expression levels were below the sensitivity of our detection method.

nCL-2 interacts with GPS1, β-COP, nm23-M2, nm23-M4, and Eya2 – To elucidate the physiological functions of nCL-2 in pit cells at the molecular level, possible nCL-2-interacting proteins were investigated. With 4.2×10^5 and 10^6 clones used as baits corresponding to domain IV and full-length nCL-2, respectively, yeast two-hybrid screening of a mouse 17-day embryo cDNA library identified 19 and 142 prey clones, respectively (table 1). Neither domain IV nor full-length nCL-2 identified 30K, whereas our previous screening of other cDNA libraries with baits corresponding to domain IV and full-length μCL isolated several 30K clones (30). A two-hybrid assay using full-length nCL-2 and 30K showed no binding under the same conditions used when μCL and mCL bound 30K (unpublished data), strongly suggesting that nCL-2 exists as a monomer/homo-oligomer without 30K, as is the case for p94 (31).

Among the molecules identified, vimentin and desmin were not focused regardless of their abundance in the obtained preys, because vimentin is not expressed in differentiated epithelial cells such as the pit cells and desmin is mainly expressed in muscle cells. Among the rests, Eyes absent homologue-2 (Eya2), G-protein pathway suppressor-1 (GPS1), nucleoside diphosphate kinases (NDPKs; nm23-M2 and -M4), translocase of outer membrane 70 (TOM70), and the β-subunit of the COPI coatomer complex (β-COP) were confirmed in their interactions with nCL-2 using a COS7 cell expression system and pull-down assays (Figs. 5E, F). It should be noted that these proteins interacted with the penta-EF-hand (PEF) domain IV of nCL-2, which is consistent with previous reports that this domain functions in the recognition of substrates and regulatory molecules (32,33,34,35).

Eya2 is one of the highly conserved vertebrate homologues of the *Drosophila eya* (*eyes absent*) gene product, required for the proper development of compound eyes. Eya2 consists of an N-terminal transactivation domain and a C-terminal Eya-conserved phosphatase domain (Fig. 5A). Yeast two-hybrid assays using truncated cDNA clones indicated that the binding site for nCL-2 is in the Eya domain (Fig. 5A). GPS1 (also called SGN1/CSN1/COPS1) is one of the subunits of the COP9 signalosome, a multifunctional protein complex conserved among eukaryotes (36). GPS1 has tricopeptide repeat (TPR) and PCI (proteasome, COP9 and eukaryotic translation initiation factor 3) domains (37,38) in the N- and C-terminal halves, respectively. The latter is the binding site for nCL-2 according to the structure identified by screening (Fig. 5B). The NDPKs, nm23-M2 and nm23-M4, are members of the nm23 family of oligomeric DNA-binding proteins with nucleoside diphosphate kinase activity. They regulate diverse cellular events including growth and differentiation, and are implicated in the pathogenesis and metastasis of tumors (39). TOM70 is a mitochondrial

protein, one of the components of the translocase of the outer membrane (TOM), and functions to import proteins destined for all submitochondrial compartments (40). TOM70 has TPR domains and several of them are binding sites for nCL-2 (Fig. 5C).

β-COP is a subunit of the coat protein I (COPI) coatomer protein complex, one representative of the intracellular vesicle coats that include COPII and clathrin. The COPI complex contains seven subunits (α-, β-, β´-, γ-, δ-, ε-, and ζ-COPs) and a small GTPase, ADP-ribosylation factor 1 (ARF1). COPI-coated vesicles are involved in protein transport within the Golgi apparatus and in retrograde selective transport from the Golgi to the ER (41). From the N-terminus, β-COP is composed of an adaptin N-terminal domain, a linker region, and a potential "ear" (also called "appendage") domain (Fig. 5D) (42,43). The ear domain is found in the C-terminal region of γ-COP, another COPI subunit. γ-COP shows high three-dimensional similarity to the C-terminal regions of α- and β-adaptins (also called α- and β-AP2), which interact with several proteins such as clathrin. Although the sequence similarity between the C-terminal regions of the β- and γ-COPs is low, they share a highly conserved FxxxW motif, suggesting the presence of a putative ear domain in β-COP (42). The structures of the isolated cDNA clones indicate that this putative ear domain is the binding site for nCL-2 (Fig. 5D).

β-COP is expressed in the proliferative and pit cells, and shows proteolytic interaction with nCL-2 – Because the expression and localization of the proteins identified above in the stomach have not yet been reported, ISH analyses were performed. The predominant expression of β-COP and Eya2 was in the upper one-third of the oxyntic mucosa and in most regions of the pyloric mucosa (Fig. 6). In contrast, the expression of GPS1, TOM70, and NDPKs was observed in the base region of the oxyntic and pyloric mucosae (unpublished data), suggesting that their localization is distinct from that of nCL-2 *in vivo*.

To investigate whether or not the observed interactions indicate that they are substrates of nCL-2, we co-expressed GPS1, NDPKs, β-COP, or Eya2 with wild-type or a protease-inactive mutant nCL-2 (C105S, active-site missense mutation) in COS7 cells. The cell lysates were then incubated with Ca^{2+} or EDTA to test for Ca^{2+}-dependent proteolysis by nCL-2. As shown in Fig. 7A, neither GPS1 (lanes 1–4), nm23-M2 (lanes 5–8), nm23-M4 (lanes 9–12), nor Eya2 (lanes 13–16) produced any proteolytic fragment, even with wild-type nCL-2 in the presence of Ca^{2+} (lanes 1, 5, 9, and 13). When β-COP was co-expressed with wild-type nCL-2 (Fig. 7B, lanes 1 and 2), proteolytic fragments were produced in a Ca^{2+}-dependent manner. Proteolysis was suppressed by the addition of inhibitors of calpain: E64c (lane 3), calpain inhibitor I (lane 4), calpeptin (lane 5), and MG132 (lane 6). Furthermore, when β-COP

was co-expressed with protease inactive nCL-2 (lanes 7 and 8), proteolysis did not occur. These results indicate that β-COP is proteolyzed directly or indirectly by nCL-2 protease activity *in vitro*.

To test whether nCL-2 directly proteolyzes β-COP, we expressed β-COP and nCL-2 in *Escherichia coli* and purified them using His-tag affinity and anion-exchange column chromatographies. When recombinant β-COP was incubated with nCL-2, two major proteolytic fragments (62 kDa and 47 kDa) of β-COP were produced in a Ca^{2+}-dependent manner (Fig. 7C, lanes 1–9, closed arrowheads), which were not detected in the sample without β-COP (lane 10). The molecular mass and the presence of the His-tag strongly suggests that the 62 kDa band corresponds to the N-terminal fragment observed in the COS7 cell experiments (Fig. 7B, lane 1, open arrowhead), and that the 47 kDa band corresponds to the remaining C-terminal fragment of β-COP. The N-terminal sequence of the 47 kDa band was determined, and β-COP was shown to be proteolyzed near the C-terminus of the adaptin N-terminal domain, between Ser528 and Ser529. Quantification of the β-COP bands clearly showed very rapid proteolysis by nCL-2 (Fig. 7C, graph).

These results indicate that β-COP is proteolyzed by nCL-2 in a Ca^{2+}-dependent manner. This is the first report of the proteolysis of β-COP. Therefore, the interactions between these molecules were further investigated.

β-COP and nCL-2 are co-localized in the Golgi – As described above, β-COP associates with COPI-coated vesicles related to the Golgi membrane, and is thus localized in the Golgi apparatus (44). When nCL-2 and β-COP were co-expressed in COS7 cells, both proteins were detected densely in the Golgi stacks, and their expression overlapped extensively (Fig. 8A, a–f). Similar localization of nCL-2 was observed in COS7 cells transfected with nCL-2 alone (Fig. 8A, g–l). To confirm the localization of nCL-2 in the Golgi, antibody directed against GM130, a *cis* Golgi marker, was used for double staining. Consistently, the expression of nCL-2 and β-COP was detected, overlapping the localization of GM130 expression (Fig. 8A, g–o). These results indicate that nCL-2 and β-COP interact in the Golgi stacks.

Identification of β-COP as an in vivo substrate of nCL-2 – To investigate the interactions between β-COP and nCL-2 under conditions similar to *in vivo* conditions, COS7 cells transfected with nCL-2 were treated with the Ca^{2+} ionophore, A23187. As shown in Fig. 8B, one major proteolytic fragment (60 kDa) of endogenous β-COP was detected only when COS cells were transfected with wild-type nCL-2 (lane 4, closed arrowhead). The molecular mass of the fragment coincided with that detected by *in vitro* proteolysis (Fig. 8C, closed arrowhead). The 60 kDa fragment was not observed when

transfected with protease-inactive nCL-2:C105S (Fig 8B, lane 6), indicating that β-COP is proteolyzed by nCL-2 in living cultured cells after stimulation with Ca^{2+} in the same manner as observed *in vitro*.

The proteolyzed fragments of β-COP were not localized to the Golgi – To investigate the physiological significance of the limited proteolysis of β-COP described above, the N- and C-terminal proteolytic fragments of β-COP (β-COP-N and -C, respectively) were expressed in COS7 cells. Immunocytochemical analysis revealed that β-COP-N and -C showed rather diffuse expression patterns that partially overlapped that of GM130 in the Golgi (Figs. 9A–I). β-COP-N and -C expressed in COS cells did not affect cell growth and viability (data not shown). These results strongly suggest that the limited proteolysis of β-COP by nCL-2 triggers translocation of the β-COP fragments from the Golgi to the cytosolic space.

DISCUSSION

In this study, we have demonstrated that the "stomach-specific" calpain nCL-2 is expressed specifically in the pit cells of the stomach and also in subsets of goblet cells in the duodenum, and that nCL-2 proteolyzes β-COP, a subunit of the COPI coatomer complex, in the Golgi upon stimulation with Ca^{2+}, resulting in the dissociation of β-COP from the Golgi. This is the first report of calpain localization in gastrointestinal tissues and of the proteolysis of the COPI subunit.

The localization of nCL-2 was strictly restricted to the pit cells in the stomach and to the goblet cells in the upper half of the villi of the duodenum. The pit and goblet cells originate from progenitor cells at the isthmus and the base region of crypts, respectively, then migrate upward to the lumen. These cells are dedicated to secreting mucus, which is one of the possible functions involving nCL-2. In the duodenum, the distributions of nCL-2 and nCL-4, the digestive-tract-specific calpains, are clearly distinct, in that nCL-4 is expressed in the goblet cells in the lower half of the villi. Although goblet cells are reported to contain several different types of cells (45,46), the distributions of these calpains suggest cell-stage, rather than cell-type, specificity, i.e., nCL-2 functions at late stages, when cells are terminally differentiated, whereas nCL-4 functions at early to mid stages, in processes including the proliferation and differentiation of cells. In the stomach, the localizations of nCL-2 and nCL-4 do not differ, except that the distribution of nCL-4 is slightly broader than that of nCL-2. This is consistent with the idea discussed above that nCL-4 functions in those cells close to the stem cells. However, the precise roles shared by these calpains must be examined further.

In contrast to the restricted localizations of nCL-2 and nCL-4 in the oxyntic mucosa, conventional ubiquitous μ- and m-calpains show rather diffuse and very little expression in this region (see Figs. 1D,

E). In the pyloric mucosa, these conventional calpains are expressed ubiquitously, and especially abundantly in the pit and the isthmus (see Figs. 2D, E). These sharp contrasts strongly suggest that the functions of the tissue-specific calpains in gastrointestinal tissues cannot be compensated by the conventional calpains, at least in the oxyntic mucosa.

Yeast two-hybrid screening followed by *in vitro* pull-down analysis identified several nCL-2-interacting proteins, including TOM70, GPS1, nm23-M2, nm23-M4, Eya2, and β-COP. ISH analysis showed that, of these, only Eya2 and β-COP are expressed in the pit cells of the oxyntic and pyloric mucosae, suggesting an *in vivo* interaction with nCL-2. Thus, the physiological significance of the observed interactions between nCL-2 and TOM70, GPS1, nm23-M2, and nm23-M4 is not clear at present. However, it should be noted that conventional calpains and skeletal-muscle-specific calpain, p94, proteolyze HSP60, a major chaperon protein in the mitochondria (47). Proteolysis of HSP60 was observed not only *in vitro*, but also in living cultured cells, suggesting a physiological significance (29). Therefore, the interaction between nCL-2 and TOM70 implies a novel but as yet unidentified function of the calpains in mitochondria.

An *in vitro* assay using a COS7 cell expression system showed that β-COP, but not Eya2, is a proteolytic substrate for nCL-2. This suggests that Eya2 is instead a regulatory and/or scaffold protein for nCL-2. Eya2 was first identified as one of the highly conserved vertebrate homologues of the *Drosophila eyes absent* gene product, required for the proper development of compound eyes. It is expressed in the cytoplasm of various tissues relatively late in mammalian development. Following its translocation to the nucleus, Eya2 forms a synergistic complex with the DNA-binding homeodomain-containing Sine oculis 1 (Six1) protein and a transcription factor, Dachshund 2 (Dach2). It thus acts as a transcriptional co-activator and its tyrosine phosphatase activity regulates specific target genes controlling cell proliferation, differentiation, and cell death during mammalian organogenesis (48,49). This study shows, for the first time, the limited expression of Eya2 in the progenitor and pit cells of the stomach. It is possible that nCL-2, binding to Eya2, is involved in gene regulation during pit cell maturation in the stomach.

The proteolytic interaction and co-localization of nCL-2 and β-COP in the Golgi strongly suggests novel functions for nCL-2 in intracellular membrane trafficking. β-COP is a subunit of the COPI coatomer complex, which coats the Golgi-derived vesicles involved in protein transport from the Golgi to the ER and within the Golgi. When a COPI-coated vesicle reaches the acceptor membrane, GTP hydrolysis by the small GTPase, ARF1, triggers coat disassembly, allowing vesicle fusion (50). The COPI complex can be reversibly dissociated into

two subcomplexes, F-COPI composed of β-, γ-, δ-, and ζ-COPs, and B-COPI composed of α-, β´-, and ε-COPs (51). Sequence similarities, as well as biochemical and structural biological properties, indicate that the F- and B-COPI complexes are significantly similar to the adaptin and clathrin complexes, respectively, other major vesicle-coating proteins involved in transport between the *trans* Golgi and the plasma membrane (42). β-COP, like γ-COP and the adaptins, can be divided into three regions: an N-terminal α-helical domain called the "adaptin N-terminal domain", a flexible linker region, and a C-terminal ear domain (see Fig. 5D).

It should be noted that the nCL-2-binding site of β-COP is in the ear domain, and that the proteolytic site of β-COP (Ser528–Ser529) is located near the boundary between the N-terminal and the linker domains (see Fig. 5D). The linker domains of β- and γ-COP bind to the WD40 repeat domains in β´-COP and α-COP, facilitating the assembly of the F- and B-COPI subcomplexes, and regulatory or accessory proteins such as AP180, eps15, amphiphysin, and epsin interact with the ear domains of the adaptins and probably with that of β-COP (42,52,53). Although the mechanisms of the disassembly of the COPI and clathrin–adaptin complexes are not fully understood, the interaction between nCL-2 and β-COP provides a new model for COPI disassembly: nCL-2, binding to the ear domain of β-COP, cleaves the linker region, causing β-COP to dissociate from the Golgi, and resulting in the irreversible disassembly of the coat proteins (Fig. 10).

This nCL-2-mediated COPI disassembly model is consistent with the report that calpain may be involved in the maturation of secretory granules via clathrin–adaptin uncoating by the limited proteolysis of clathrin and the adaptins (54). Moreover, the relationship between membrane trafficking and the calpains has been confirmed recently, e.g., calpain localization in the ER and Golgi (55), in lipid rafts (56), and in multivesicular bodies (57) etc., suggesting a general involvement of various calpains in a variety of membrane trafficking processes. Continued anterograde protein transport in the secretory pathway is tightly coupled with COPI-mediated retrograde, retrieval transport system. The stomach is an "extreme" environment where the pH is extremely low and many infective microorganisms enter, and extensive protection by a tough mucosa is thus essential. To ensure the quality and amount of glycoproteins secreted from the mucosa, such as mucins, a secretion system that includes retrograde transport has to function at full capacity. This may be one reason why the stomach has an additional COPI disassembly system involving nCL-2. The different levels of expression of nCL-2 in the intestines and trachea, in which the mucosa is also very important, possibly explain the requirement for this extra secretion system in the stomach, mediated by

nCL-2, in addition to the usual system.

It is also possible that, like Eya2, β-COP functions as a scaffold protein for nCL-2 in its proteolysis of substrates as yet unidentified. One of the most important questions is how calpain selects specific substrates for proteolysis. A scaffold for proteolysis, like that observed in various kinase cascades, is a strong possibility, although there are few reports of scaffold proteins for calpain (30,58). These possibilities can be explored in mice genetically modified at the gene for nCL-2. This research is now proceeding in our laboratory.

REFERENCES

1. Sorimachi, H., and Suzuki, K. (2001) *J. Biochem.* **129**, 653-664.
2. Goll, D. E., Thompson, V. F., Li, H., Wei, W., and Cong, J. (2003) *Physiol. Rev.* **83**, 731–801.
3. Suzuki, K., Hata, S., Kawabata, Y., and Sorimachi, H. (2004) *Diabetes* **53**, S12–18.
4. Hosfield, C. M., Elce, J. S., Davies, P. L., and Jia, Z. (1999) *EMBO J.* **18**, 6880–6889.
5. Strobl, S., Fernandez-Catalan, C., Braun, M., Huber, R., Masumoto, H., Nakagawa, K., Irie, A., Sorimachi, H., Bourenkow, G., Bartunik, H., Suzuki, K. and Bode, W. (2000) *Proc. Natl. Acad. Sci. USA* **97**, 588–592.
6. Hata, S., Sorimachi, H., Nakagawa, K., Maeda, T., Abe, K., and Suzuki, K. (2001) *FEBS Lett.* **501**, 111–114.
7. Moldoveanu, T., Hosfield, C. M., Lim, D., Elce, J. S., Jia, Z., and Davies, P. L. (2002) *Cell* **108**, 649–660.
8. Arthur, J. S., Elce, J. S., Hegadorn, C., Williams, K., and Greer, P. A. (2000) Disruption of the murine calpain small subunit gene, Capn4: calpain is essential for embryonic development but not for cell growth and division. *Mol. Cell. Biol.* **20**, 4474–4481.
9. Richard, I., Broux, O., Allamand, V., Fougerousse, F., Chiannilkulchai, N., Bourg, N., Brenguier, L., Devaud, C., Pasturaud, P., Roudaut, C., Hillaire, D., Passos-Bueno, M., Zatz, M., Tischfield, J. A., Fardeau, M., Jackson, C. E., Cohen, D. and Beckmann, J. S. (1995) *Cell* **81**, 27–40.
10. Horikawa, Y., Oda, N., Cox, N. J., Li, X., Orho-Melander, M., Hara, M., Hinokio, Y., Lindner, T. H., Mashima, H., Schwarz, P. E., del Bosque-Plata, L., Horikawa, Y., Oda, Y., Yoshiuchi, I., Colilla, S., Polonsky, K. S., Wei, S., Concannon, P., Iwasaki, N., Schulze, J., Baier, L. J., Bogardus, C., Groop, L., Boerwinkle, E., Hanis, C. L. and Bell, G. I. (2000) *Nat. Genet.* **26**, 163–175.
11. Denison, S. H., Orejas, M., and Arst, Jr. H. N. (1995) *J. Biol. Chem.* **270**, 28519–28522.
12. Barnes, T. M., and Hodgkin, J. (1996) *EMBO J.* **15**, 4477–4484.
13. Futai, E., Maeda, T., Sorimachi, H., Kitamoto, K., Ishiura, S., and Suzuki, K. (1999) *Mol. Gen. Genet.* **260**, 559-568.
14. Syntichaki, P., Xu, K., Driscoll, M., and Tavernarakis, N. (2002) *Nature* **419**, 939–944.
15. Lid, S. E., Olsen, L., Nestestog, R., Aukerman, M., Brown, R. C., Lemmon, B., Mucha, M., Opsahl-Sorteberg, H. G., and Olsen, O. A. (2005) *Planta* **221**, 339-351.
16. Sorimachi, H., Ishiura, S., and Suzuki, K. (1993) *J. Biol. Chem.* **268**, 19476–19482.
17. Hata, S., Nishi, K., Kawamoto, T., Lee, H. J., Kawahara, H., Maeda, T., Shintani, Y., Sorimachi, H., and Suzuki, K. (2001) *J. Mol. Evol.* **53**, 191–203.
18. Duan, W. R., Ito, M., Lee, E. J., Chien, P. Y., and Jameson, J. L. (2002) *Biochem. Biophys. Res. Commun.* **295**, 261–266.

19. Cao, Y., Zhao, H., and Grunz, H. (2001) *Dev. Growth Differ.* **43**, 563–571.
20. Lee, H. J., Sorimachi, H., Jeong, S. Y., Ishiura, S., and Suzuki, K. (1998) *Biol. Chem.* **379**, 175–183.
21. Liu, K., Li, L., and Cohen, S. N. (2000) *J. Biol. Chem.* **275**, 31093–31098.
22. Yoshikawa, Y., Mukai, H., Hino, F., Asada, K., and Kato, I. (2000) *Jpn. J. Cancer Res.* **91**, 459–463.
23. Yao, X., Thibodeau, A., and Forte, J. G. (1993) *Am. J. Physiol.* **265**, C36–46.
24. Lee, E. R., Trasler, J., Dwivedi, S., and Leblond, C. P. (1982) *Am. J. Anat.* **164**, 187–207.
25. Karam, S. M., and Leblond, C. P. (1993) *Anat. Rec.* **236**, 259–279.
26. Karam, S. M., Straiton, T., Hassan, W. M., and Leblond, C. P. (2003) *Stem Cells* **21**, 322–336.
27. Hattori, T., and Fujita, S. (1976) *Cell Tissue Res.* **175**, 49–57.
28. Masumoto, H., Yoshizawa, T., Sorimachi, H., Nishino, T., Ishiura, S., and Suzuki, K. (1998) *J. Biochem.* **124**, 957–961.
29. Sorimachi, H., Toyama-Sorimachi, N., Saido, T. C., Kawasaki, H., Sugita, H., Miyasaka, M., Arahata, K., Ishiura, S., and Suzuki, K. (1993) *J. Biol. Chem.* **268**, 10593–10605.
30. Kimura, E., Abe, K., Suzuki, K., and Sorimachi, H. (2003) *Biosci. Biotechnol. Biochem.* **67**, 1786–1796.
31. Sorimachi, H., Kinbara, K., Kimura, S., Takahashi, M., Ishiura, S., Sasagawa, N., Sorimachi, N., Shimada, H., Tagawa, K., Maruyama, K. and Suzuki, K. (1995) *J. Biol. Chem.* **270**, 31158–31162.
32. Noguchi, M., Sarin, A., Aman, M.J., Nakajima, H., Shores, E. W., Henkart, P. A., and Leonard, W. J. (1997) *Proc. Natl. Acad. Sci. USA* **94**, 11534–11539.
33. Shinozaki, K., Maruyama, K., Kume, H., Tomita, T., Saido, T. C., Iwatsubo, T., and Obata, K. (1998) *Int. J. Mol. Med.* **1**, 797–799.
34. Benetti, R., Del Sal, G., Monte, M., Paroni, G., Brancolini, C., and Schneider, C. (2001) *EMBO J.* **20**, 2702–2714.
35. Bordone, L., and Campbell, C. (2002) *J. Biol. Chem.* **277**, 26673–26680.
36. Tsuge, T., Matsui, M., and Wei, N. (2001) *J. Mol. Biol.* **305**, 1–9.
37. Hofmann, K., Bucher, P. (1998) *Trends Biochem. Sci.* **23**, 204–205.
38. Han, D. S., Kim, H. S., Jang, W. H., Lee, S. D., and Suh, J. K. (2004) *Nucleic Acids Res.* **32**, 6312–6320.
39. Postel, E. H. (1998) *Int. J. Biochem. Cell Biol.* **30**, 1291–1295.
40. Beddoe, T., Bushell, S. R., Perugini, M. A., Lithgow, T., Mulhern, T. D., Bottomley, S. P., and Rossjohn, J. (2004) *J. Biol. Chem.* **279**, 46448–46454.
41. Wieland, F., and Harter, C. (1999) *Curr. Opin. Cell Biol.* **11**, 440–446.
42. Hoffman, G. R., Rahl, P. B., Collins, R. N., and Cerione, R. A. (2003) *Mol. Cell* **12**, 615–625.
43. Watson, P. J., Frigerio, G., Collins, B. M., Duden, R., and Owen, D. J. (2004) *Traffic* **5**, 79–88.

44. Presley, J. F., Ward, T. H., Pfeifer, A. C., Siggia, E. D., Phair, R. D., and Lippincott-Schwartz, J. (2002) *Nature* **417**, 187–193.
45. Oliver, M. G., and Specian, R. D. (1991) *Anat. Rec.* **230**, 513–518.
46. Nieuw Amerongen, A. V., Bolscher, J. G., Bloemena, E., and Veerman, E. C. (1998) *Biol. Chem.* **379**, 1–18.
47. Ono, Y., Kakinuma, K., Torii, F., Irie, A., Nakagawa, K., Labeit, S., Abe, K., Suzuki, K., and Sorimachi, H. (2004) *J. Biol. Chem.* **279**, 2761–2771.
48. Li, X., Oghi, K. A., Zhang, J., Krones, A., Bush, K. T., Glass, C. K., Nigam, S. K., Aggarwal, A. K., Maas, R., Rose, D. W. and Rosenfeld, M. G. (2003) *Nature* **426**, 247–254.
49. Rayapureddi, J. P., Kattamuri, C., Steinmetz, B. D., Frankfort, B. J., Ostrin, E. J., Mardon, G., and Hegde, R. S. (2003) *Nature* **426**, 295–298.
50. Lanoix, J., Ouwendijk, J., Lin, C. C., Stark, A., Love, H. D., Ostermann, J., and Nilsson, T. (1999) *EMBO J.* **18**, 4935–4948.
51. Lowe, M., and Kreis, T. E. (1995) *J. Biol. Chem.* **270**, 31364–31371.
52. Owen, D. J., Vallis, Y., Noble, M. E., Hunter, J. B., Dafforn, T. R., Evans, P. R., and McMahon, H. T. (1999) *Cell* **97**, 805–815.
53. Traub, L. M., Downs, M. A., Westrich, J. L., and Fremont, D. H. (1999) *Proc. Natl. Acad. Sci. USA* **96**, 8907–8912.
54. Ohkawa, K., Takada, K., Asakura, T., Hashizume, Y., Okawa, Y., Tashiro, K., Ueda, J., Itoh, Y., and Hibi, N. (2000) *Neuroreport* **11**, 4007–4011.
55. Hood, J. L., Brooks, W. H., and Roszman, T. L. (2004) *J. Biol. Chem.* **279**, 43126–43135.
56. Morford, L. A., Forrest, K., Logan, B., Overstreet, L. K., Goebel, J., Brooks, W. H., and Roszman, T. L. (2002) *Biochem. Biophys. Res. Commun.* **295**, 540–546.
57. Xu, W., Smith, F. J., Subaran, R., and Mitchell, A. P. (2004) *Mol. Biol. Cell* **15**, 5528–5537.
58. Gotthardt, M., Hammer, R. E., Hubner, N., Monti, J., Witt, C. C., McNabb, M., Richardson, J. A., Granzier, H., Labeit, S., and Herz, J. (2003) *J. Biol. Chem.* **278**, 6059–6065.

Acknowledgements

We are grateful to Keiji Tanaka, Tomoki Chiba, Shigeo Murata, Choji Taya, and Hiromichi Yonekawa at Rinshoken, Toshiyuki Takeuchi (Gunma University), Taeko Dohi (International Medical Center of Japan), Shoichi Ishiura and Ichiro Matsumoto (University of Tokyo), and all of our laboratory members for experimental support and valuable discussion. This work was supported in part by MEXT.KAKENHI 16026209 (to HS), 14704064, 15032201, and 16026201 (to HK), 14086203 (to TM), 14380309 (to KS), and 14656054 (to KA), by JSPS.KAKENHI 15380089

(to HS) and 02J07250 (to SH), by a Research Grant (14B-4) for Nervous and Mental Disorders from the Ministry of Health, Labor and Welfare, and by Ground-Based Research Announcement for Space Utilization promoted by JSF (to HS).

The abbreviations used are: nCL-2, novel calpain large subunit-2; nCL-4, novel calpain large subunit-4; COP, coat protein; ISH, *in situ* hybridization; NP-40, nonidet p-40.

FIGURE LEGENDS

Fig. 1. Expression of calpain mRNAs in the mouse stomach oxyntic mucosa. (A) Schematic structures of the mouse stomach corpus (oxyntic) mucosa. Serial sections of mouse oxyntic mucosa were hybridized with Dig-labeled nCL-2 (B), nCL-4 (C), μCL (D), and mCL (E) riboprobes. The hybridization signals were analyzed by phase contrast microscopy. No signal was observed with control sense riboprobes (unpublished data). Bars, 100 μm.

Fig. 2. Expression of calpain mRNAs in the mouse stomach pyloric mucosa. (A) Schematic structures of the mouse stomach pyloric mucosa. Serial sections of mouse pyloric mucosa were hybridized with Dig-labeled nCL-2 (B), nCL-4 (C), μCL (D), and mCL (E) riboprobes. Bars, 100 μm.

Fig. 3. Specific expression of nCL-2 in the pit cells. (A) Schematic structures of nCL-2 and nCL-2′, and the locations of epitopes for the antibodies used. (B) Protein (20 μg) from mouse gastric mucosa was analyzed by western blotting probed with anti-nCL2/2′ antibody. The arrowhead indicates the band corresponding to nCL-2. nCL-2′ (43 kDa) was not detected. (C–F) Sections of rat stomach oxyntic mucosa were immunostained with anti-nCL2/2′ (C, E, and F) and anti-nCL2C (D) antibodies. Signals were visualized by Alexa 594 (C and D) or HRP methods (E and F). (F) A magnified image of the area indicated by the broken square in (E). Arrowheads in (F) indicate nCL-2-negative parietal cells. (G and H) Rat oxyntic mucosa sections immunostained with anti-nCL2/2′ (red) and anti-H^+/K^+-ATPase (green) antibodies (G), or with anti-nCL2/2′ (red) and anti-PCNA (green) antibodies (H). Staining with secondary antibody alone yielded negligible background signal in all experiments (unpublished data). Bars, 100 μm.

Fig. 4. Expression of nCL-2 in subsets of goblet cells in the duodenum. (A) Northern blot analysis of various mouse (lanes 1–9) and human (lanes 10–33) tissues using the probes indicated. Lanes: 1, testis; 2 and 24, skeletal muscle; 3 and 29, liver; 4 and 28, kidney; 5 and 32, lung; 6, 13, and 22, brain; 7, large intestine; 8 and 17, stomach; 9 and 30, small intestine; 10, adrenal grand; 11, bladder; 12, bone marrow; 14, lymph node; 15, prostate; 16, spinal cord; 18, thyroid; 19, tongue; 20, trachea; 21, uterus; 23, heart; 25, colon; 26, thymus; 27, spleen; 31, placenta; 33, peripheral blood leukocytes. (B and C) ISH analysis of mouse duodenum sections was performed using riboprobes for nCL-2 (B) and nCL-4 (C). The lower two panels are magnified images of the upper panels. (D) Immunostaining of the rat duodenum using anti-nCL2/2′ antibody. Arrows indicate nCL-2 immunoreactive goblet cells characterized by their expanded shape in the apical region. L, lumen; E, epithelium; LP, lamina propria. Bars, 100 μm (B and C), 50 μm (D).

Fig. 5. Identification of nCL-2-interacting proteins. Schematic structures of nCL-2-binding proteins identified by yeast two-hybrid screening using domain IV and full-length nCL-2 as baits: Eya2 (A), GPS1 (B), TOM70 (C), β-COP (D). Thick lines below the schematic structures indicate the positions and lengths of the identified prey clones (see table 1). Thin lines in (A) indicate two truncated constructs used to examine the binding site for Eya2; + and – stand for the binding and unbinding of the fragment to nCL-2, respectively, examined with a yeast two-hybrid system. The closed arrowhead in (D) indicates the proteolytic site of β-COP (see Fig. 7). (E) HA-tagged GPS1 (lanes 1 and 2), β-COP (lanes 3 and 4), nm23-M2 (lanes 5 and 6), nm23-M4 (lanes 7 and 8), and Eya 2 (lanes 9 and 10) were transfected with FLAG-tagged nCL-2 (odd lanes) or mock vector (even lanes) into COS7 cells. The cell lysates were immunoprecipitated with anti-FLAG agarose, and subjected to western blot analysis using anti-FLAG and anti-HA monoclonal antibodies. (F) GST (lane 2) or GST-fusion protein (lane 3) of the C-terminal region of TOM70 corresponding to the identified two-hybrid clone (see (A)) was incubated with FLAG-tagged nCL-2:C105S expressed in COS7 cells, and pulled-down by glutathione–Sepharose. Lane 1 shows 10% of the input of FLAG-nCL-2:C105S.

Fig. 6. Expression of nCL-2-interacting proteins, GPS1 and β-COP, in mouse stomach pit cells. β-COP (A and C) and Eya2 (B and D) transcripts were expressed in the pit cells of the mouse stomach oxyntic (A and B) and pyloric (C and D) mucosae, demonstrated by ISH. For the structure of the stomach section, see Figs. 1 and 2. Bars, 100 μm.

Fig. 7. Proteolytic interaction of β-COP, but not GPS1, nm23-M2, -M4, or Eya2, with nCL-2. (A) HA-tagged GPS1 (lanes 1–4), nm23-M2 (lanes 5–8), nm23-M4 (lanes 9–12), or Eya 2 (lanes 13–16) were co-transfected into COS7 cells with FLAG-tagged WT or protease-inactive mutant nCL-2 (CS), and the cell lysates were incubated with or without Ca^{2+} as indicated. Bands were detected by western blot analysis using anti-HA antibody. Closed arrowheads and asterisks indicate the full-length proteins and non-specific bands, respectively. (B) HA-tagged β-COP was transfected into COS7 cells with FLAG-tagged WT (lanes 1–6) or protease-inactive mutant nCL-2 (CS, lanes 7 and 8), and the cell lysates were incubated with (lanes 1 and 3–7) or without (lanes 2 and 8) Ca^{2+} in the absence (lanes 1, 2, 7, and 8) or presence of 50 μM E64c (lane 3), 10 μM calpain inhibitor I (lane 4), 10 μM calpeptin (lane 5), or 10 μM MG132 (lane 6). Bands were detected by western blot analysis using anti-HA antibody. Closed and open arrowheads indicate full-length β-COP and a proteolytic fragment of β-COP, respectively. Asterisks indicate non-specific bands. (C) (upper) Recombinant β-COP was incubated with or without recombinant nCL-2 in the absence or presence of Ca^{2+} as indicated (lane 10 did not contain β-COP), and stained by CBB. The closed arrow, open

and closed arrowheads indicate β-COP, nCL-2, and proteolytic fragments of β-COP, respectively. Asterisks indicate unrelated proteins co-purified with β-COP. (lower) The intensity of the 62 kDa band was quantified by densitometry. Values were means ± SD; n = 3.

Fig. 8. Co-localization of nCL-2 with β-COP in the Golgi, and limited proteolysis of β-COP after Ca^{2+}-ionophore stimulation. (A) COS7 cells transfected with FLAG-tagged nCL-2 (a–l), HA-tagged β-COP (a–f), or mock vector (m–o) were doubly immunostained with anti-nCL2C (red) and anti-HA antibodies (green) (a–f), with anti-nCL2C (red) and anti-GM130 (green) antibodies (g–l), or with anti-β-COP (red) and anti-GM130 antibodies (green) (m–o). The merged images show overlapping signals for nCL-2 and β-COP (c and f), nCL-2 and GM130 (i and l), and β-COP and GM130 (o) in the perinuclear region corresponding to the Golgi. The cells shown here are representative of the ones most frequently observed. N, nucleus. Bars, 20 μm.
(B) COS7 cells transfected with mock vector (lanes 1 and 2), FLAG-tagged nCL-2 (lanes 3 and 4), or FLAG-tagged nCL-2:C105S (lanes 5 and 6) were treated with dimethylsulfoxide (lanes 1, 3, and 5), or 10 μM A23187 (lanes 2, 4, and 6) for 20 hr, and detected by western blot analysis using anti-β-COP antibody. An arrow and an arrowhead indicate endogenous β-COP and its proteolytic fragment, respectively. (C) Lysate of COS7 cells transfected with FLAG-tagged nCL-2, was incubated with or without Ca^{2+}, and compared with the sample same as in Fig. 8B lane 4. An arrow and an arrowhead indicate endogenous β-COP and its proteolytic fragment, respectively, detected by western blot analysis using anti-β-COP antibody.

Fig. 9. The proteolyzed fragment of β-COP localized dispersed from the Golgi. COS7 cells transfected with HA-tagged β-COP (full-length), β-COP-N (aa 1–528), or β-COP-C (aa 529–953), respectively, were doubly immunostained with anti-HA (A, D, and G; red) and anti-GM130 (B, E, and H; green) antibodies. β-COP-N and -C showed rather diffuse expression patterns that partially overlapped with that of GM130 in the Golgi (C, F, and I). The cells shown here are representative of the ones most frequently observed. N, nucleus. Bars, 20 μm.

Fig. 10. Schematic illustration of a proposed model for COPI disassembly. A model of the disassembly of the COPI subcomplex with proteolysis by nCL-2, modified from the model proposed by Hoffman *et al.* (42). nCL-2 binds to the ear domain of β-COP through domain IV and also to possible regulatory molecule(s) such as Eya2. Upon stimulation with Ca^{2+}, nCL-2 proteolyzes β-COP close to the C-terminal end of the adaptin N-terminal domain to dissociate the polymeric COPI complex to the single complex.

Table 1. Summary of the results of yeast two-hybrid screening

Bait	Prey	Count	*In vitro* Interaction[a]
domain IV	nucleotide diphosphate kinase nm23-M2	12	+
	β-subunit of COPI coatomer (β-COP)	2	+
	translocase of outer membrane 70 (TOM70)	2	+
	nucleotide diphosphate kinase nm23-M3	1	n.d.[b]
	eyes absent homologue 2 (Eya2)	1	+
	G-protein pathway suppressor 1 (GPS1)	1	+
total		19	
full-length	vimentin	77	n.d.
	desmin	25	n.d.
	nm23-M2	3	+
	nucleotide diphosphate kinase nm23-M4	3	+
	Eya2	2	+
	hemopoietic lineage switch protein 5 (Hls5)	2	n.d.
	β-COP	1	+
	GPS1	1	+
	pre-B cell leukemia transcription factor interacting protein 1 (Pbxip1)	1	n.d.
	hemoglobin α	1	n.d.
	axotrophin	1	n.d.
	tyrosine kinase-associated leucine zipper protein	1	n.d.
	Nedd9	1	n.d.
	cardiac actin	1	n.d.
	perlican	1	n.d.
	aldo-keto reductase	1	n.d.
	RIKEN cDNA clone 3632410O17	1	n.d.
	RIKEN cDNA clone 4932411G06	1	n.d.
	(unidentified sequence)	18	n.d.
total		142	

[a] For *in vitro* interactions, see Figs. 5E and F. [b] n.d., not determined.

Hata *et al.*, Figure 1

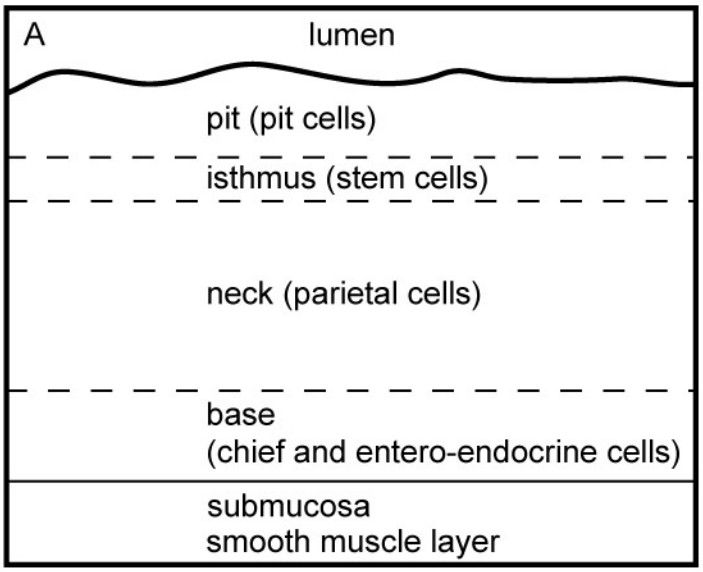

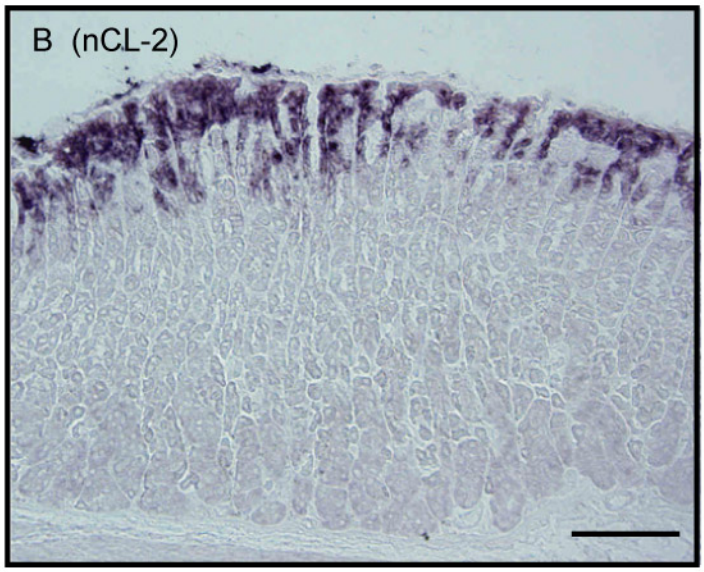

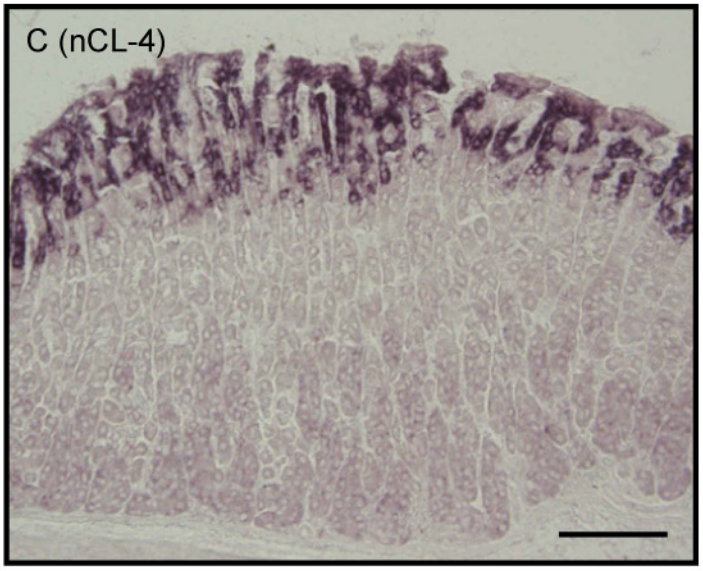

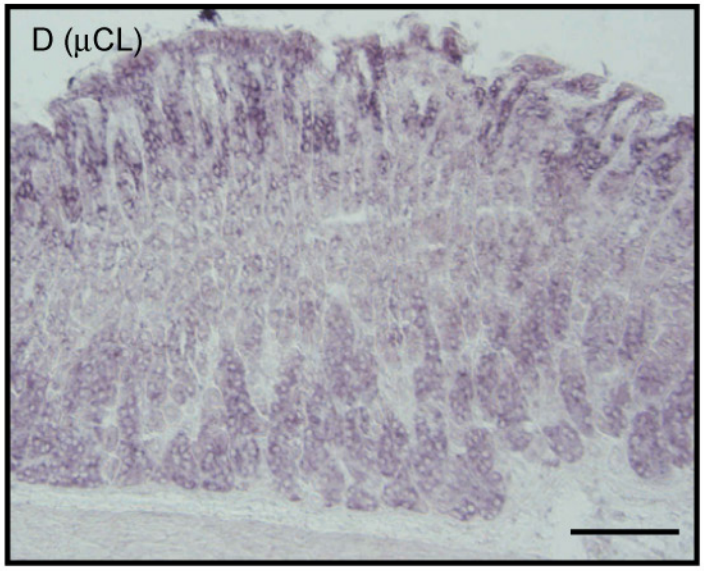

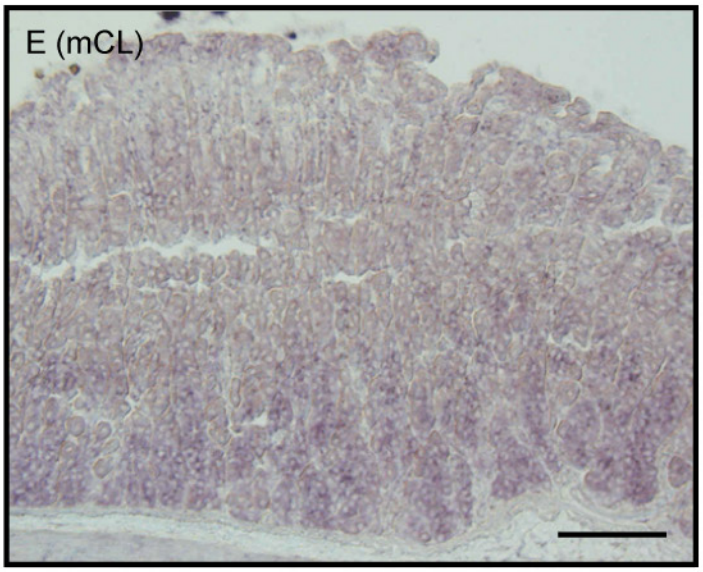

Hata *et al.*, Figure 2

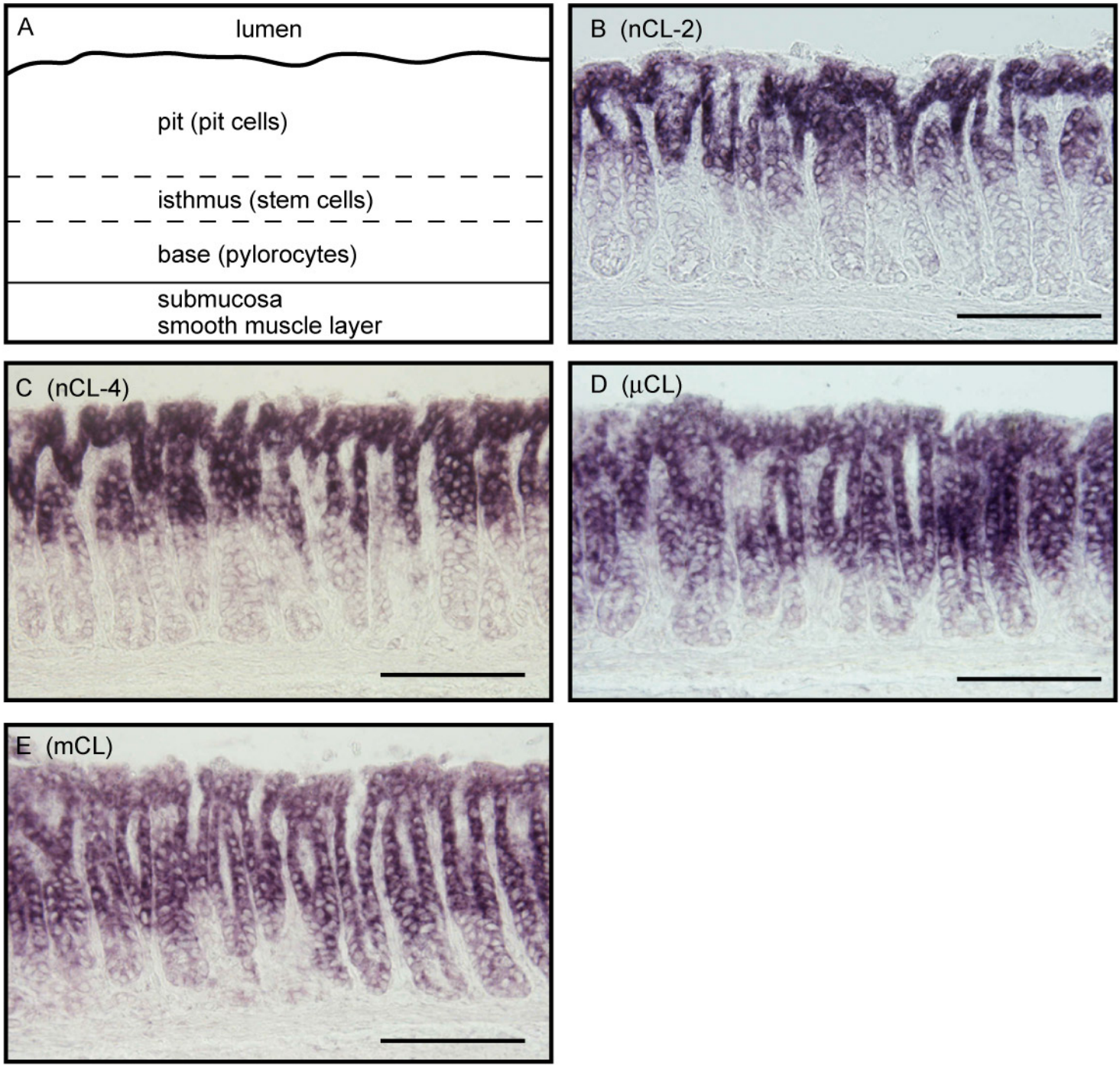

Hata *et al*., Figure 3

(A)

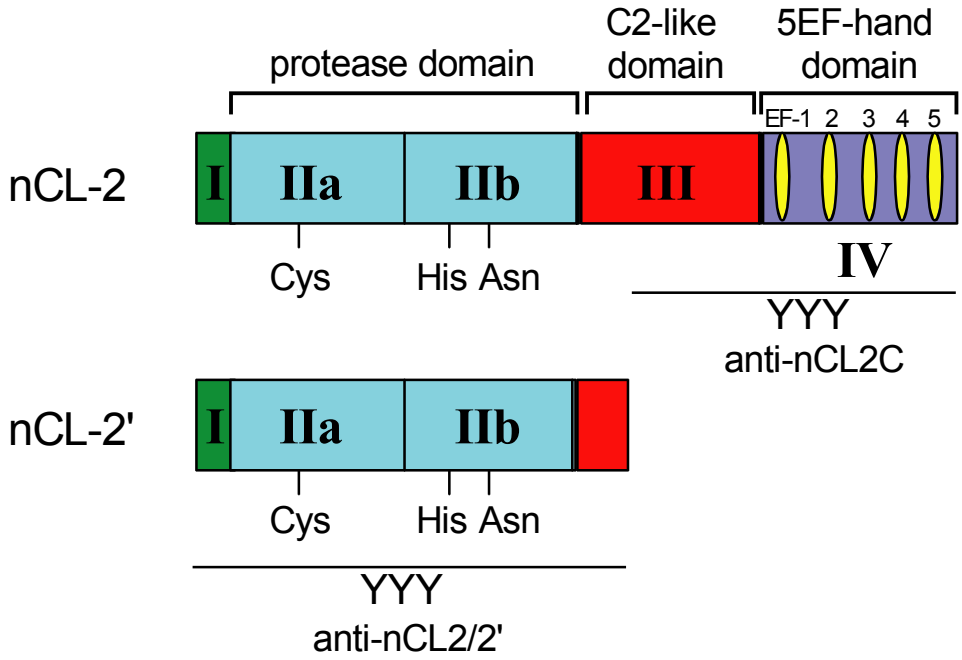

(B)

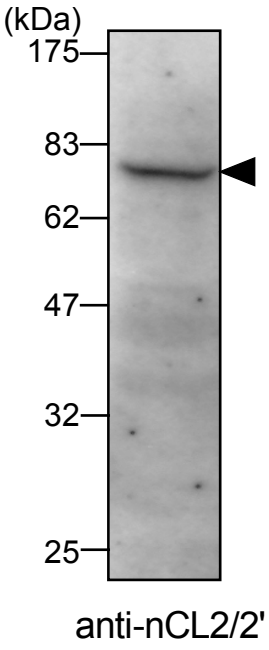

Hata *et al*., Figure 3 (continued)

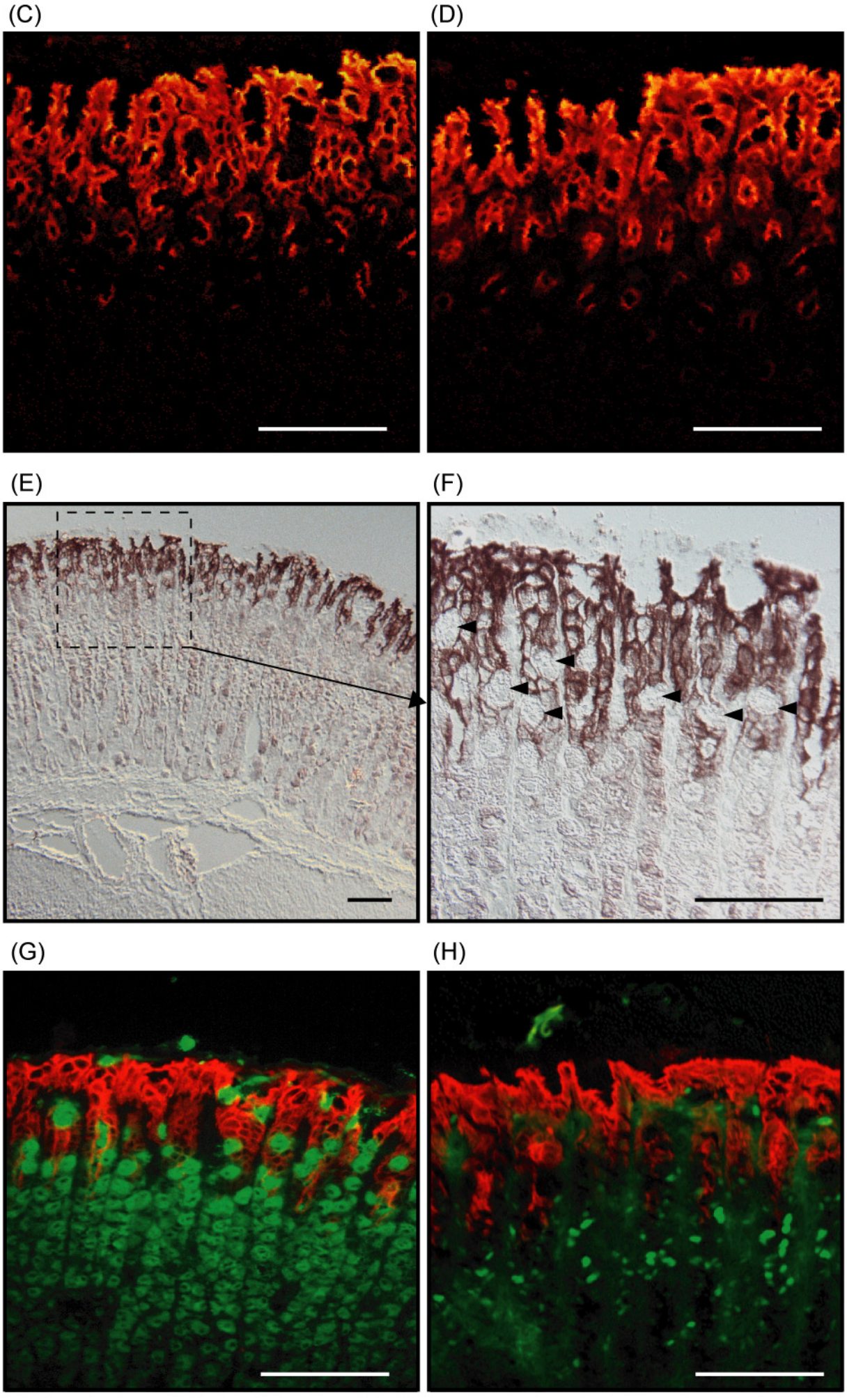

Hata *et al*., Figure 4

(A)

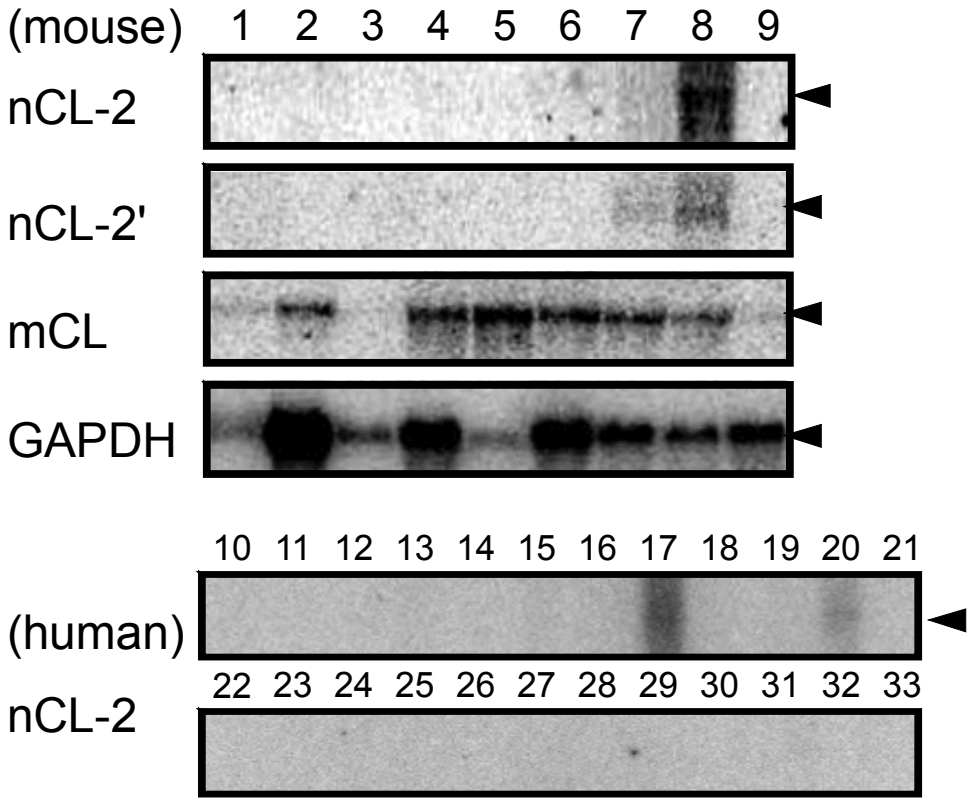

Hata *et al.*, Figure 4 (continued)

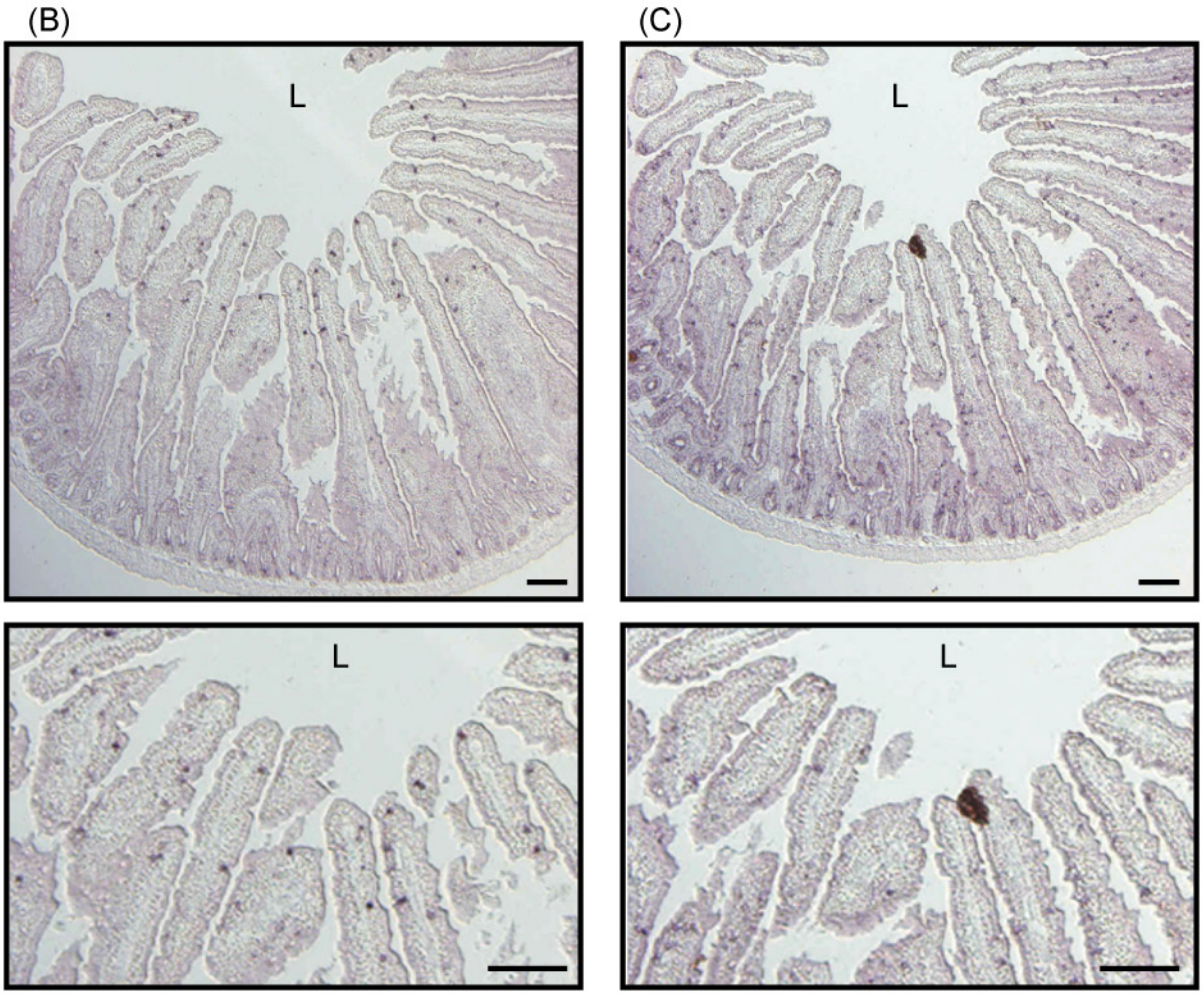

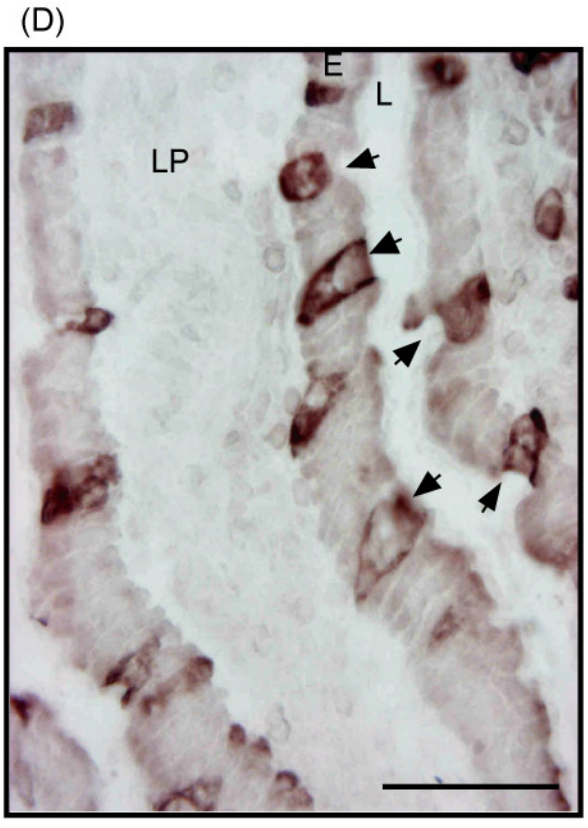

Hata *et al*., Figure 5

(A)

(Eya2)

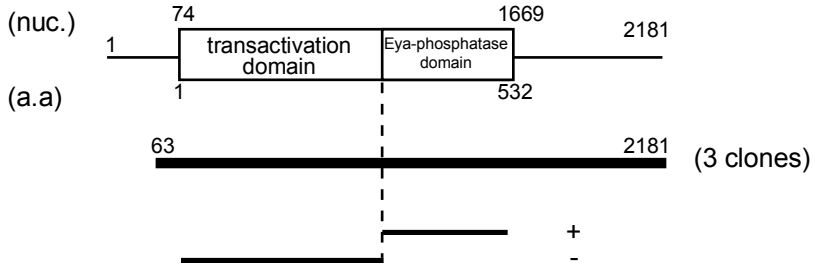

(B)

(GPS1)

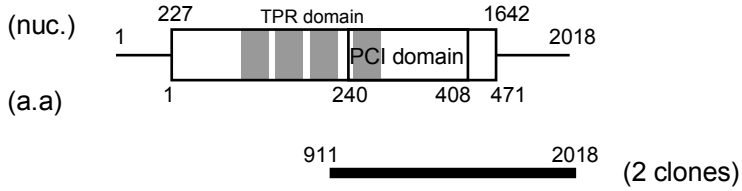

(C)

(TOM70)

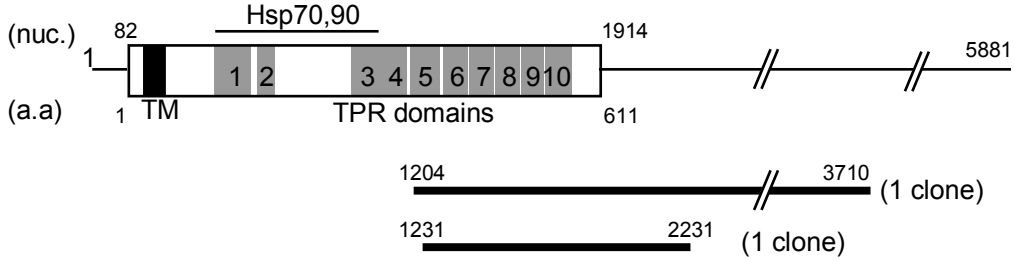

(D)

(β-COP)

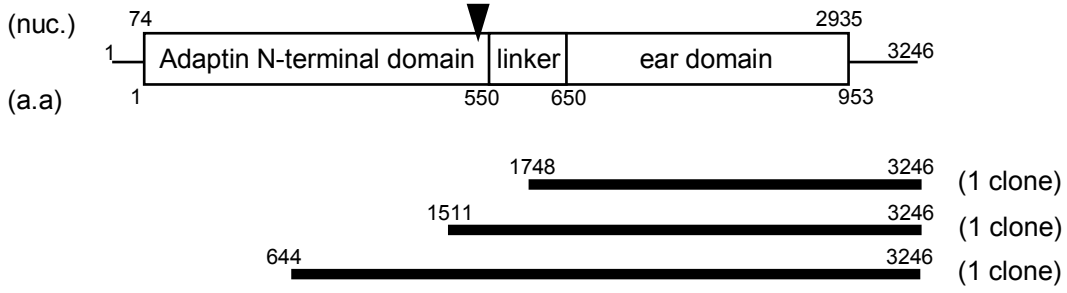

Hata *et al*., Figure 5 (continued)

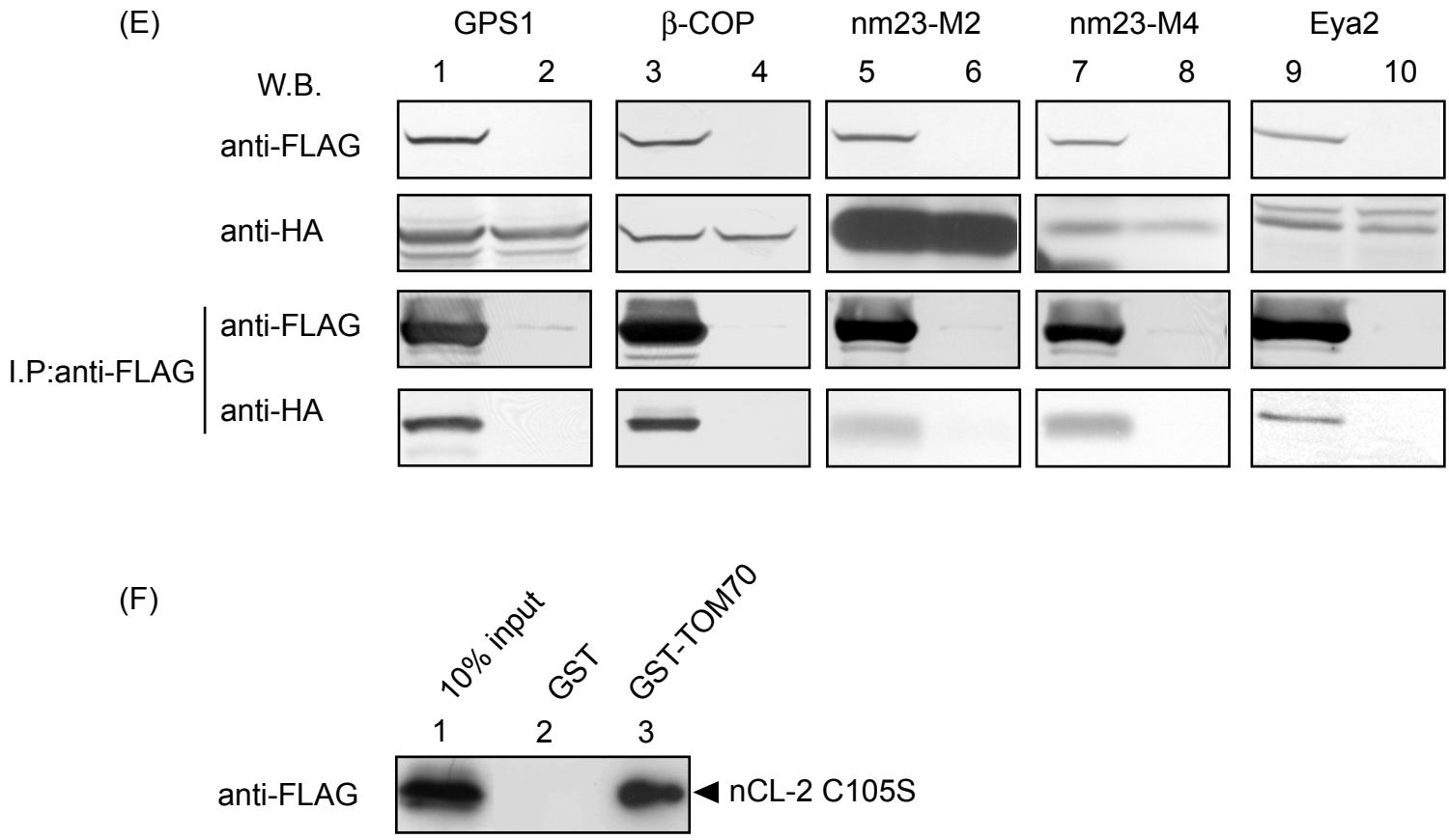

Hata *et al*., Figure 6

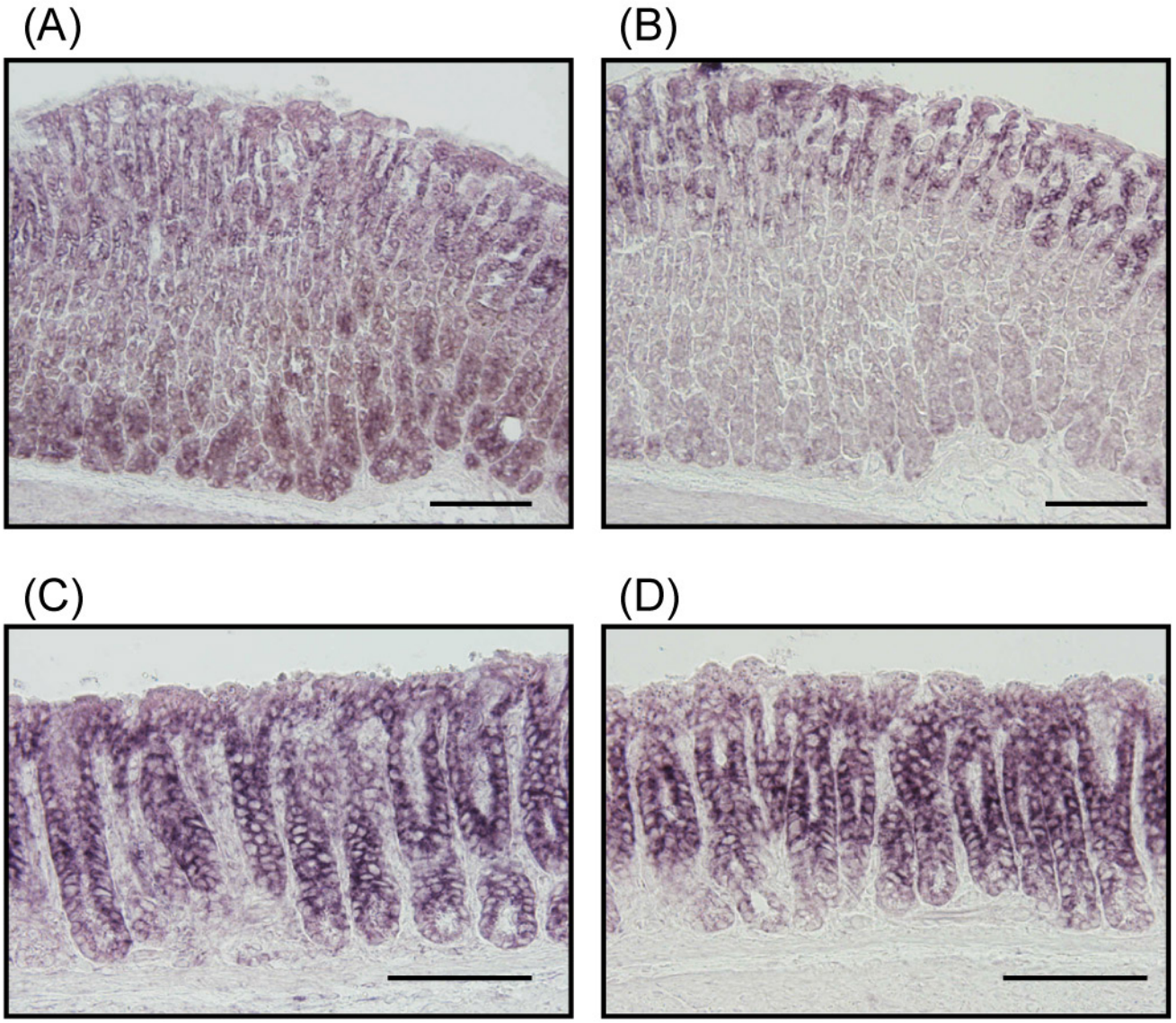

Hata *et al*., Figure 7

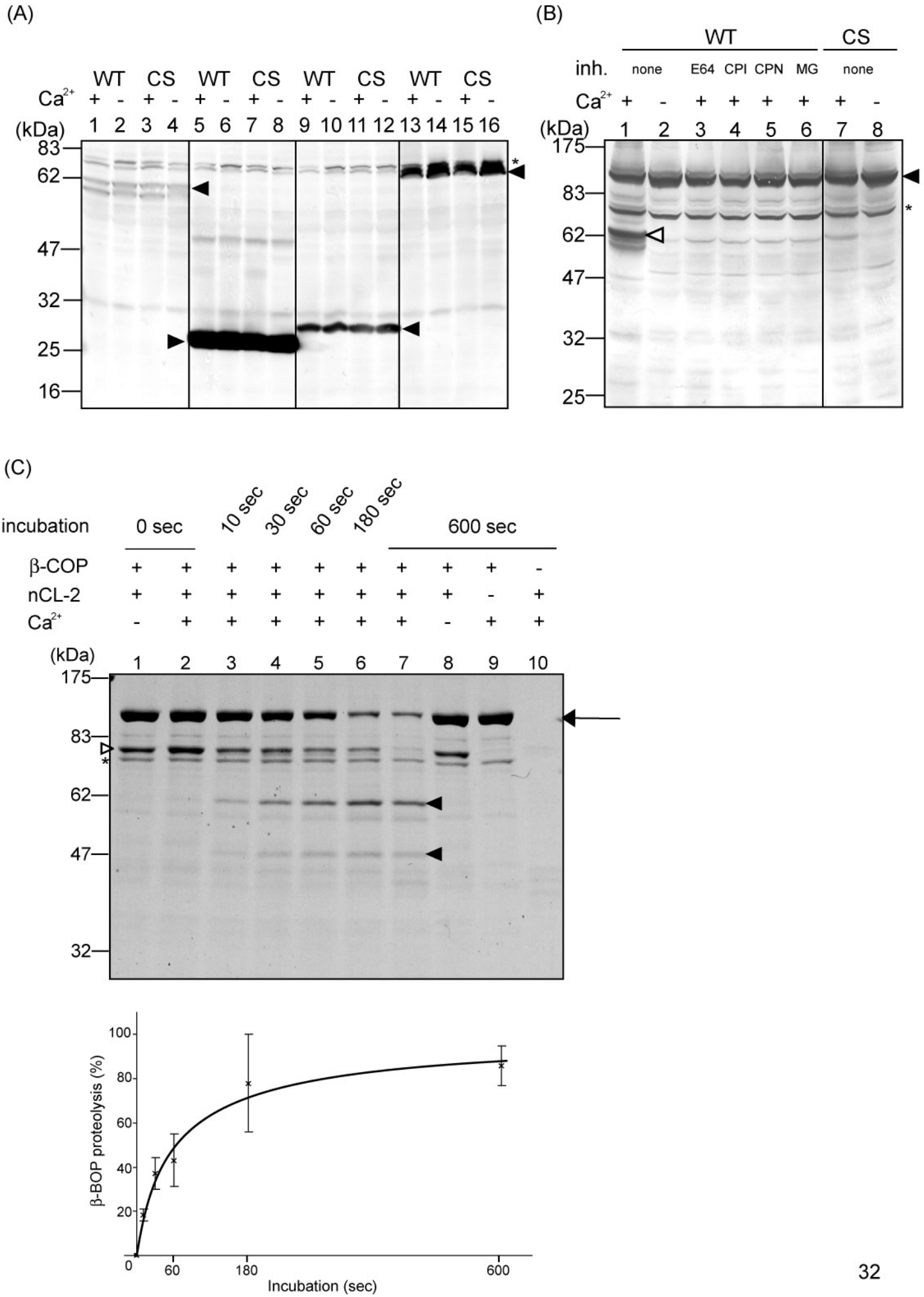

Hata *et al.*, figure 8

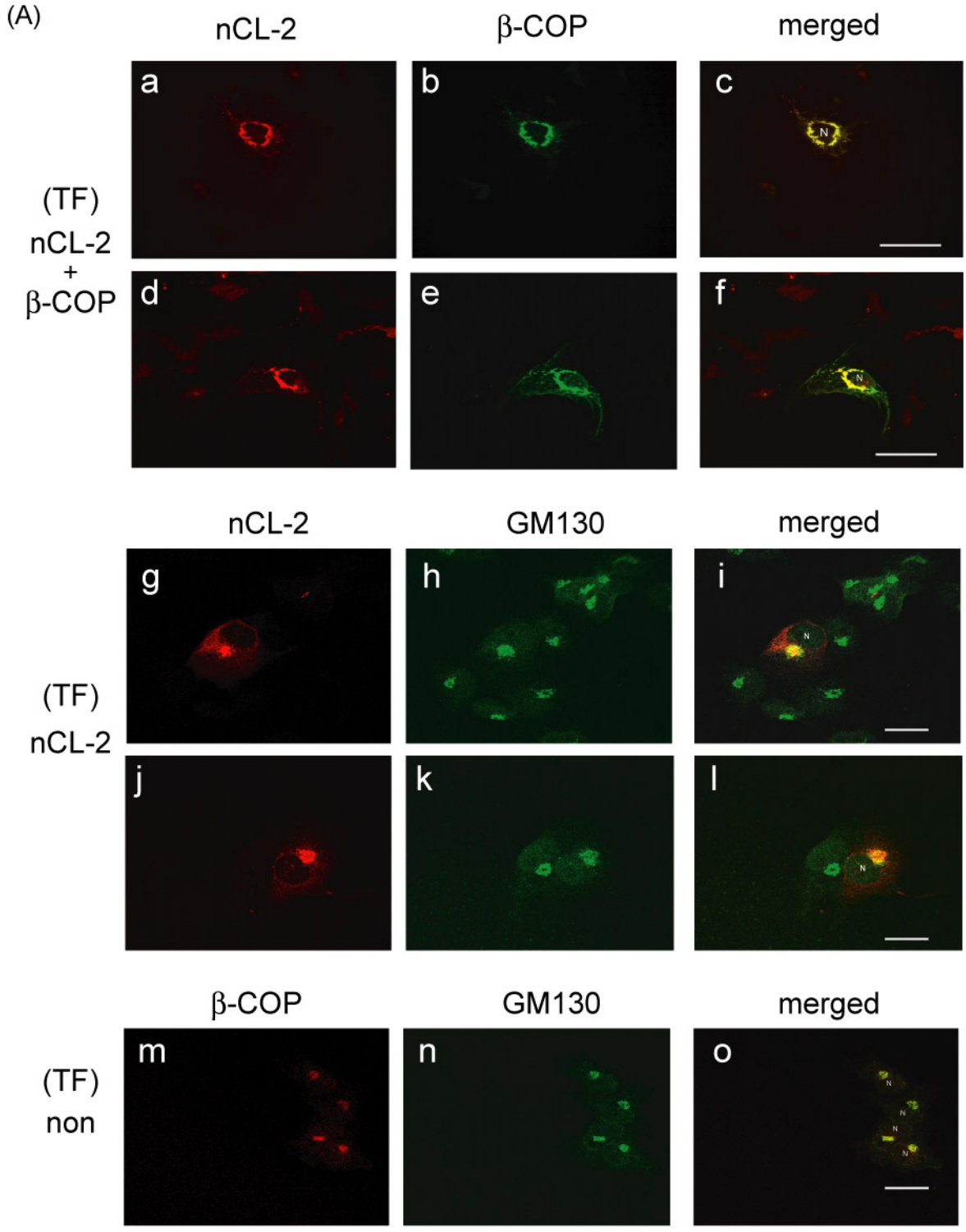

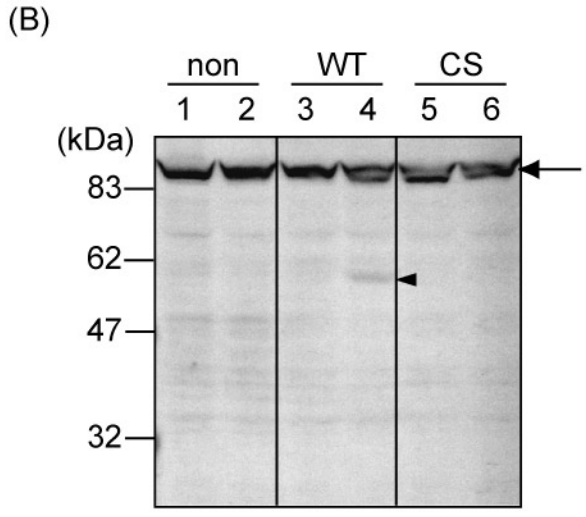

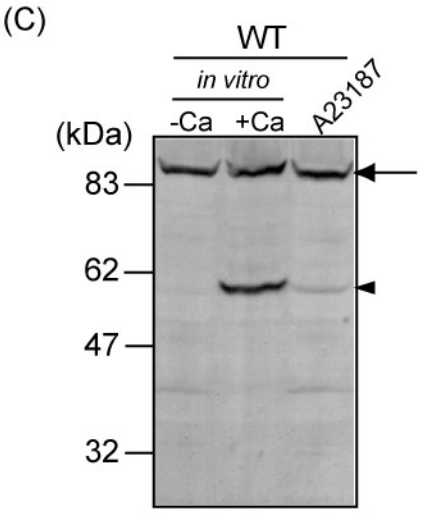

Hata *et al.*, Figure 9

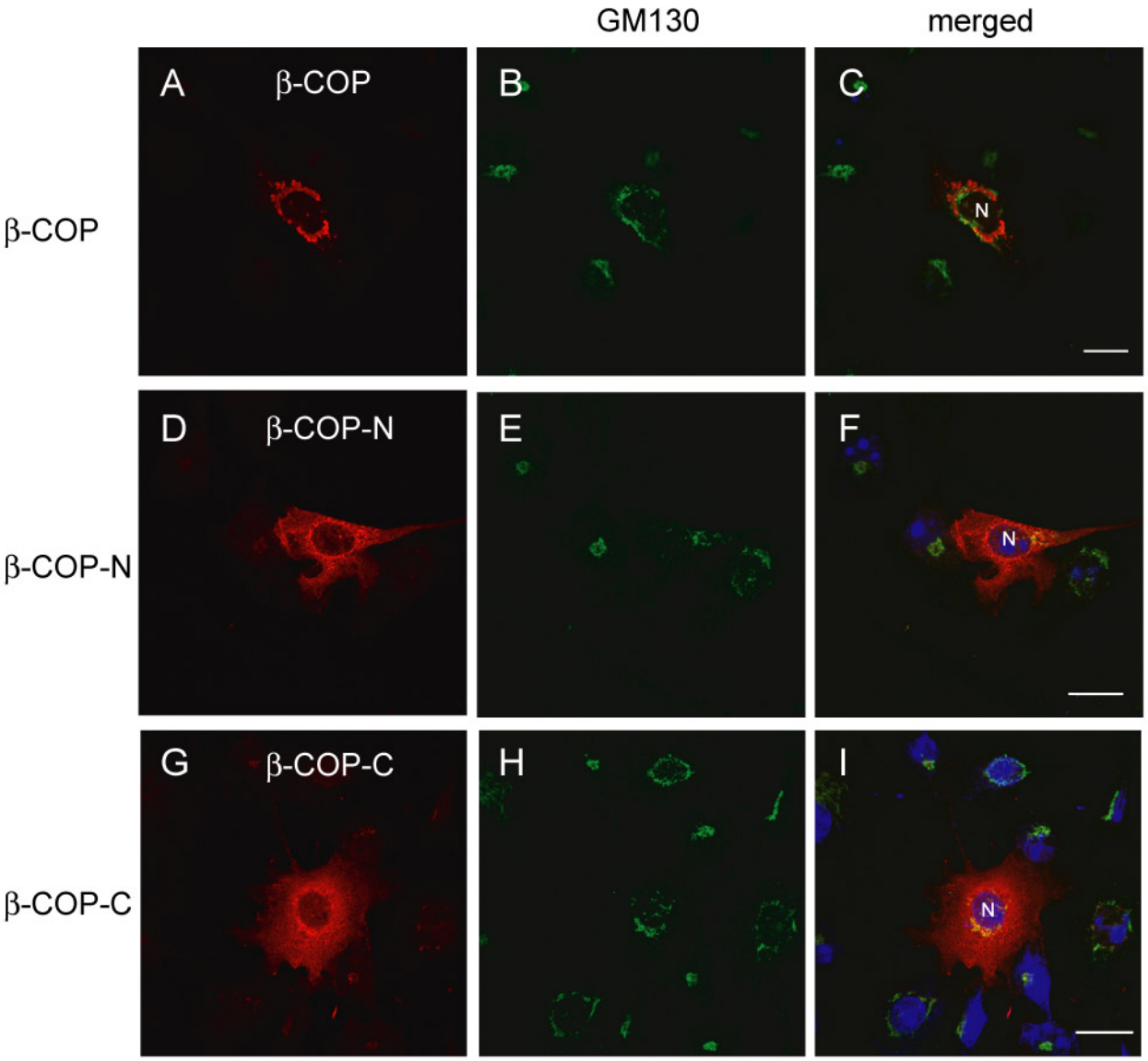

Hata *et al*., Fig. 10